NASA/TM–2018-219027/ Vol. 1

PACE Technical Report Series
Volume 1

Ivona Cetinić, Charles R. McClain, and P. Jeremy Werdell, Editors

ACE Ocean Working Group recommendations and instrument requirements for an advanced ocean ecology mission

National Aeronautics and
Space Administration

Goddard Space Flight Center
Greenbelt, Maryland 20771

February 2018

NASA STI Program ... in Profile

Since its founding, NASA has been dedicated to the advancement of aeronautics and space science. The NASA scientific and technical information (STI) program plays a key part in helping NASA maintain this important role.

The NASA STI program operates under the auspices of the Agency Chief Information Officer. It collects, organizes, provides for archiving, and disseminates NASA's STI. The NASA STI program provides access to the NASA Aeronautics and Space Database and its public interface, the NASA Technical Report Server, thus providing one of the largest collections of aeronautical and space science STI in the world. Results are published in both non-NASA channels and by NASA in the NASA STI Report Series, which includes the following report types:

- TECHNICAL PUBLICATION. Reports of completed research or a major significant phase of research that present the results of NASA Programs and include extensive data or theoretical analysis. Includes compilations of significant scientific and technical data and information deemed to be of continuing reference value. NASA counterpart of peer-reviewed formal professional papers but has less stringent limitations on manuscript length and extent of graphic presentations.
- TECHNICAL MEMORANDUM. Scientific and technical findings that are preliminary or of specialized interest, e.g., quick release reports, working papers, and bibliographies that contain minimal annotation. Does not contain extensive analysis.
- CONTRACTOR REPORT. Scientific and technical findings by NASA-sponsored contractors and grantees.
- CONFERENCE PUBLICATION. Collected papers from scientific and technical conferences, symposia, seminars, or other meetings sponsored or co-sponsored by NASA.
- SPECIAL PUBLICATION. Scientific, technical, or historical information from NASA programs, projects, and missions, often concerned with subjects having substantial public interest.
- TECHNICAL TRANSLATION. English-language translations of foreign scientific and technical material pertinent to NASA's mission.

Specialized services also include organizing and publishing research results, distributing specialized research announcements and feeds, providing help desk and personal search support, and enabling data exchange services. For more information about the NASA STI program, see the following:

- Access the NASA STI program home page at http://www.sti.nasa.gov
- E-mail your question via the Internet to help@sti.nasa.gov
- Phone the NASA STI Information Desk at 757-864-9658
- Write to:
  NASA STI Information Desk
  Mail Stop 148
  NASA's Langley Research Center
  Hampton, VA 23681-2199

NASA/TM–2018-219027/ Vol. 1

PACE Technical Report Series
Volume 1

Ivona Cetinić, Charles R. McClain, and P. Jeremy Werdell, Editors

ACE Ocean Working Group recommendations and instrument requirements for an advanced ocean ecology mission

National Aeronautics and
Space Administration

Goddard Space Flight Center
Greenbelt, Maryland 20771

February 2018

Level of Review: This material has been technically reviewed by technical management.

Available from

NASA STI Program
Mail Stop 148
NASA's Langley Research Center
Hampton, VA 23681-2199

National Technical Information Service
5285 Port Royal Road
Springfield, VA 22161
703-605-6000

Available in electronic form at http://

INTRODUCTION

Introduction to this volume and series

The Plankton, Aerosol, Cloud, ocean Ecosystem (PACE; https://pace.gsfc.nasa.gov) mission represents NASA's next great investment in satellite ocean color and the combined study of Earth's ocean-atmosphere system. At its core, PACE builds upon NASA's multi-decadal legacies of the Coastal Zone Color Scanner (1978-1986), Sea-viewing Wide Field-of-view Sensor (SeaWiFS; 1997-2010), Moderate Resolution Imaging Spectroradiometers (MODIS) onboard Terra (1999-present) and Aqua (2002-present), and Visible Infrared Imaging Spectroradiometer (VIIRS) onboard Suomi NPP (2012-present) and JPSS-1 (2017-present; to be renamed NOAA-20). The ongoing, combined climate data record from these instruments changed the way we view our planet and – to this day – offers an unparalleled opportunity to expand our senses into space, compress time, and measure life itself.

This volume marks the first in new NASA Technical Report series that will document the scientific activities of and the supporting formulation decision criteria for the PACE mission. As demonstrated by the SeaWiFS Project, such a series ensures the availability of critical information on the mission, instruments, and algorithms to the scientific community. The PACE Project hopes this series will continue and build upon spirit of openness and collaboration within the community begun by the SeaWiFS Technical Report series over 25 years ago. The second volume will present the PACE Science Definition Team Report (originally released in 2012). At the time of this writing, we are actively preparing additional volumes, as well – one on scientific analyses and activities related to mission architecture, another on mission and instrument requirements, and another on spectrometer design – all of which were conducting during mission phases Pre-Phase A (2014-2016; pre-formulation: define a viable and affordable concept) and Phase A (2016-2017; concept and technology development). The mission entered Phase B (preliminary design and technology completion) in July 2017. We chose to use these first two volumes, however, to present material that predates the mission itself, offering insight into how PACE came to be.

While NASA Headquarters officially realized the PACE mission in January 2014, the idea of PACE extends back well over a decade. Formulation of PACE science objectives and instrument requirements commenced in 2000 with a NASA agency-wide carbon cycle initiative that spanned ocean, land, and atmosphere disciplines. Over time, the concept of an advanced ocean biology mission matured into what has become PACE, with much of the evolution occurring under the auspices of the Aerosol, Cloud, and ocean Ecosystems (ACE; 2008-present) mission. The ACE ocean working group, in particular, poured substantial effort into mission formulation and derivation of requirements for an advanced space-borne spectroradiometer that advanced the legacies of SeaWIFS and MODIS. In the end, the PACE Project views this ACE ocean white paper as the first documentation of the vision, science rationale and measurement requirements of what has become the PACE mission. With that in mind, we (the PACE Project) are deeply indebted to the ACE ocean working group and, accordingly, present their white paper as the first volume of the PACE Technical Report series.

P. J. Werdell
PACE Project Scientist
November 2017

Introduction to this volume

Our Earth is home to over seven billion people. The ocean covers 71% of the Earth's surface, and global Earth observing satellites allow us to see a view of our Earth and its ocean about every two days. The beauty of our ocean planet is profound and its importance to humanity, our health, and economy is staggering. As of 2010, 80% of the world's population lives within 60 miles of a coast. Fourteen percent of U.S. counties that are adjacent to the coast produce 45 percent of the nation's gross domestic product (GDP), with close to three million jobs (one in 50) directly dependent on the resources of the oceans and the Great Lakes. The Food and Agriculture Organization of the United Nations estimates that fisheries and aquaculture assure the livelihoods of 10-12 percent of the world's population, with more than 90 percent of those employed by capture fisheries working in small-scale operations in developing countries. From jobs to food to recreation to regulating climate, the ocean is vital to all life on Earth.

The advent of satellite oceanography in the late 1970's allowed Earth scientists to have a wide-angle lens with which to view the vast expanses of life near the ocean's surface. Complementing ship-based snapshots of the ocean's biology and chemistry, satellites provided an ability to have a global, long-term view of the ocean from space. The Earth's aquatic realm is immense, and prior to satellite observations the oceans remained critically undersampled in time and space. Methods that improve the temporal and spatial coverage offset this problem and infallibly lead to major leaps in our understanding of the oceans. The partnership between in-water (e.g., ship, mooring, drifter) and satellite ocean sampling is essential and must, at a minimum, persist so we can understand and protect our home planet. Such measurements are particularly critical during the current era of varying and rapidly changing climate. Explosive growth of human populations along coastal margins places increasing pressure on dynamic coastal and aquatic ecosystems, modifying natural processes and, in many cases, putting life, health, and property at risk from hazards inherent to the ocean.

Ocean color remote sensing began with the launch of the Coastal Zone Color Scanner (CZCS) proof-of-concept mission in 1978. What have CZCS and other ocean color data revealed? To start, we have confirmed that a close coupling exists between ocean climate and primary production. We know that the biologically productive ocean is extremely sensitive to vertical mixing. We have also verified the general Sverdrup/Riley concepts: that the combination of vertical mixing and light in a water column has major effects on the seasonal and temporal appearance of phytoplankton in the ocean. Satellite data of the ocean also allow ready identification of ocean and coastal fronts, which are key sites of high productivity and support tremendous upper trophic level biomass. Global ocean satellite data have also improved our understanding of important interactive relationships between coastal (e.g. squirts, jets, eddies) and oceanic waters, revealing a far greater influence of coastal processes on global ocean basins than anticipated. A global ocean view has additionally enabled previously unattainable synoptic estimates of primary production that can be resolved seasonally and decadally.

In mid-September of 2007, the ocean research community achieved a major milestone as NASA and industry partners marked the collection of ten uninterrupted years of global Sea-viewing Wide Field-of-view Sensor (SeaWiFS) satellite ocean color data. Discovery and confirmation of oceanographic phenomena from ocean color continued with SeaWiFS, and included the impact of sunlight absorption by phytoplankton on the heat budget of the ocean, and elucidation of the linkage between biological production, associated carbon fixation, and climate. These findings and others concerning light penetration, photosynthesis, and phytoplankton growth within the oceans confirmed ideas that were established long before satellites existed. However, the use of satellites grounded these theories concerning the ocean biosphere and placed these theories within the context of Earth's global ecology.

The ten-year time series of SeaWiFS data allows researchers to take the pulse of Earth's living oceans on a global scale in near-real time. Ten years beyond that and with a range of international ocean color missions and sensors, we now find ourselves standing on the threshold of possible breakthroughs in ocean biological and chemical sciences. Critical to this progress have been advances in our understanding of ocean circulation and cryospheric science aided by additional satellite observations. These data streams support research needs as well as applications (internationally) with regard to defense, fisheries management, environmental and water quality, shipping, and recreation.

The decade of global, research-quality satellite ocean color data is a significant achievement and rightly celebrated. However, as a community devoted to the stewardship of Earth, we must emphasize the need for a sustained, long-term commitment to continuous, global, research quality colorimetric observations. Despite the profound advances already achieved in understanding our ocean gardens, much of the global ocean remains unexplored and its ecology a mystery. We have a responsibility to continue today's minimum set of key climate observations of ocean biology and chemistry. There is also a clear path to move international ocean color remote sensing well beyond current capabilities and begin exploring new questions and enabling new discoveries regarding our ocean gardens.

The past three decades have given us only a brief glimpse of a constantly changing Earth system in which natural and human factors interplay. We know that ocean ecosystems and their biogeochemical cycles are extremely complex. It is therefore incumbent upon us to inspire and support the next generation of satellites and Earth scientists. Discoveries await in Earth's living oceans. Our path may lead to insights on global change, some perhaps we have not yet considered. However, the time series of satellite ocean color data to provide the basis of future exploration and enable both these discoveries and climate research is not guaranteed.

To gain insight in to climate variability and change, one requirement is a continuous time series of observations to estimate ocean properties such as phytoplankton chlorophyll a with the radiometric accuracy of SeaWiFS or better. Describing and quantifying new properties of ocean biology and chemistry from satellites allows developments in basic research, such as the mechanistic understanding of phytoplankton physiology, habitat health, and carbon fluxes, to move from the laboratory to the global context of Earth's biosphere. These advances require an evolution in satellite instruments and missions beyond traditional measurements that enable scientific discovery. And it is here that the challenge lies; to ensure that developments in ocean color remote sensing match the rapid pace of scientific research.

Without global ocean color satellite data, humanity loses its capacity to take Earth's pulse and to explore its unseen world. It is our duty to provide a long-term surveillance system for the Earth, not only to understand and monitor the Earth's changing climate, but to enable the next generations of students to make new discoveries in our ocean gardens as well as explore similar features on other planets.

This technical report series is the product of these efforts. It outlines a strategy for the international community to lead in the scientific application of remote sensing technologies for the exploration and understanding of biological and biogeochemical processes of our oceans. This effort is absolutely critical to ensure the sustainability of our ocean economy, protect our home planet, and inspire the next generation of explorers and scientists, mathematicians and writers. The vision is to fully discover the mechanisms and interactions that sustain life on our ocean planet, reaching for new heights technologically, and revealing the unknown for the benefit of humankind.

P. S. Bontempi
PACE Program Scientist
November 2017

ACE Ocean White Paper TM preface

Formulation of science objectives and sensor requirements for an advanced ocean biology satellite mission began in 2000 with a NASA agency-wide carbon cycle initiative that included ocean, terrestrial, and atmospheric disciplines [*Gervin et al.*, 2002; *McClain et al.*, 2002]. Details on an advanced ocean biology mission matured over a series of subsequent studies:

- The Physiology-Multispectral Mission (PhyLM) was developed in 2004 at the NASA Goddard Space Flight Center (GSFC) in preparation for an expected NASA Pathfinder opportunity. PhyLM was a 2-instrument concept and included an aerosol lidar. We were the co-PIs. The solicitation was never released.
- The Ocean Carbon, Ecology and Near-Shore (OCEaNS) mission concept was presented at NASA Headquarters in 2005 and then submitted as a mission concept white paper to the National Research Council Earth Sciences Decadal Survey (NESDS) solicitation by ourselves and Jay Herman (NASA GSFC). OCEaNS was a 3-instrument concept and included an aerosol lidar and a polarimeter.
- The Global Ocean Carbon, Ecosystems, and Coastal Processes (GOCECP, 2006) mission was a study requested by NASA Headquarters in response to the NESDS. The GOCECP study was conducted at NASA GSFC with one key objective to estimate the cost of an advanced ocean color mission (ocean sensor only). We were the science leads for that study.
- *The Earth's Living Ocean*, a report by the NASA Ocean Biology and Biogeochemistry Working Group [2007] on mission priorities for the ocean biology and biogeochemistry program organized and lead by Paula Bontempi, the NASA program manager. We were members of the working group.
- The Aerosol, Cloud, and ocean Ecosystems (ACE, 2008-present) mission was recommended by the NESDS. The ACE mission was initially a 4-instrument mission including an advanced ocean color sensor, aerosol lidar, and a polarimeter (consistent with the OCEaNS mission concept), plus a dual-frequency cloud radar. Hal Maring and Paula Bontempi were the Headquarters program scientists. We served as leads for the ocean science component of ACE. The ACE ocean white paper, published herein, was drafted in 2010 with the final version submitted to the ACE program scientists in 2011. Similar white papers were submitted by the aerosol, cloud, and ocean-atmosphere interaction working groups.

One outcome of the ACE mission studies was the Pre-ACE concept, where the two passive sensors (ocean radiometer and polarimeter) would be launched earlier than the active sensors (lidar and radar). The idea was that the passive sensors were more mature in their development and would likely have sufficiently long lifetimes that the active sensors (with anticipated shorter lifetimes) could be launched somewhat later to create the desired constellation of simultaneous observations from all four instruments.

In 2010, NASA released the document *Responding to the Challenges of Climate and Environmental Change [NASA, 2010]* which, among other recommendations, called for a "highly calibrated Ocean Ecosystem Spectroradiometer (OES)" co-manifested with a multi-spectral and multi-angle polarimeter. This Pre-ACE mission concept was renamed as the Plankton, Aerosol, Cloud, ocean Ecosystem (PACE) mission. The PACE mission was directed to GSFC in late 2014.

We suggested to Jeremy Werdell, PACE Project Scientist, that the ACE ocean white paper be published as a NASA Technical Memorandum by the PACE Project because the white paper is the first documentation of the science rationale, objectives, and measurement requirements of what has become the PACE mission. The ACE ocean working group devoted much time and thought into mission

formulation. We believe these contributions are reflected in the ACE white paper and deserve publication in an official, citable document.

M. J. Behrenfeld and C. R. McClain

ACE Ocean Working Group Leads

November 2017

Contents

Chapter 1

ACE Ocean Ecosystems

ACE Ocean Working Group, November 2011

1.1. Introduction

The Earth's ecosystems are comprised of a myriad of physical, chemical, biological and ecological processes that create a variety of adaptive and resilient communities of organisms on both the land and in the sea. These ecosystems are an integral part of the planet's biogeochemical cycles (e.g., carbon, nitrogen, phosphorous, silica, iron, etc.), which, in turn, are coupled to and influence the planet's climate through feedback processes, many of which are not clearly understood. With the advent of satellite ocean color technology, the global distribution of marine biosphere properties such as chlorophyll concentration, water clarity, primary production, particle concentrations, and others can be routinely surveyed and monitored over time. The data have been used, along with other biological and hydrographic data, to identify ocean biogeochemical provinces and to define the ecological geography of the ocean [*Longhurst*, 1998]. These capabilities, along with improved measurements at sea and numerical models of ocean circulation and ecosystem dynamics, are revolutionizing our understanding of the marine biosphere and how it interacts with the rest of the Earth system. The ACE ocean science objectives represent a major advance in ocean ecosystem and biogeochemical research and require a huge step forward from traditional satellite ocean color measurement capabilities. In this chapter, the science objectives and rationale are outlined as are the commensurate measurement requirements.

The Carbon Cycle

In outlining the ACE mission, the Decadal Survey highlighted the need for continued measurement of marine primary production to refine estimates of the air-sea exchange of CO_2 and its long-term CO_2 sequestration in the deep ocean. Implicit in this requirement is the need to understand how marine ecosystems are changing and the corresponding temporal changes in the distribution and composition of phytoplankton and the processes that are regulating these. Figure 1.1 depicts the global carbon cycle with current estimates of the terrestrial, oceanic, and atmospheric reservoirs and fluxes. The deep ocean is, by far, the largest reservoir of carbon readily available to the "active" component of the carbon cycle. Of course, there are larger reservoirs in sedimentary rock formations and other geological deposits, but these are essentially unavailable except via the extraction and use of fossil fuels as shown in Figure 1.1. The net uptake of carbon by both the terrestrial and oceanic systems is relatively small representing the difference between much larger fluxes. Estimates of biological CO_2 incorporation through net primary production are similar (~50 GtC/yr) for global terrestrial and ocean systems, and are approximately matched by concurrent respiratory CO_2 production and export to the deep sea. The

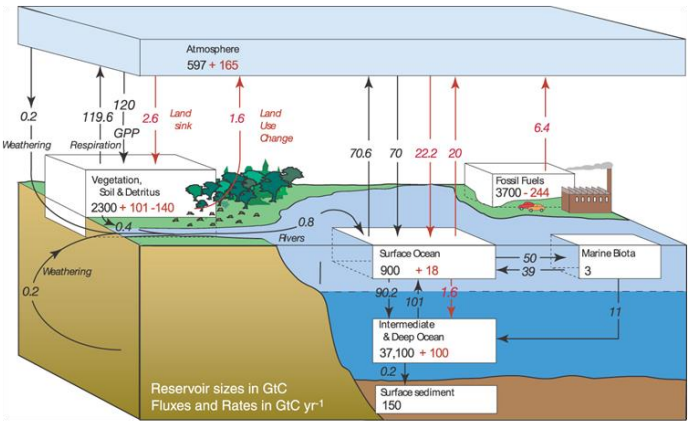

Figure 1.1. Global Carbon Cycle (modified from IPCC [2007]).

anthropogenic CO_2 source is 6.4 GtC/yr, with roughly half of this annual flux sequestered by ocean and terrestrial systems. Ocean uptake is mediated through exchange with the overlying atmosphere, so as atmospheric CO_2 concentrations rise, the ocean concentration adjusts accordingly; but ocean uptake is tied to the ocean's bicarbonate system. Ocean biology modulates the bicarbonate system primarily through the uptake of CO_2 by photosynthesis. The surface equilibrium is disrupted by exchanges of carbon with the deep ocean. These exchanges [Figure 1.1] are driven by ocean circulation (water mass subduction and convection) and the sinking particle fluxes (the so-called "biological pump"). As Figure 1.2 implies, the carbon pathways and transformations in the ocean are complex and depth dependent. Satellite observations are critical for measuring bio-optical and chemical properties near the surface and models are essential to understanding how ocean ecological processes ultimately modulate the air-sea fluxes and the exchanges with the deep ocean leading to the long-term sequestration of fossil fuel CO_2. Achieving an accurate quantification of the distribution, composition, and vertical fluxes of particles is a key objective of the ACE mission.

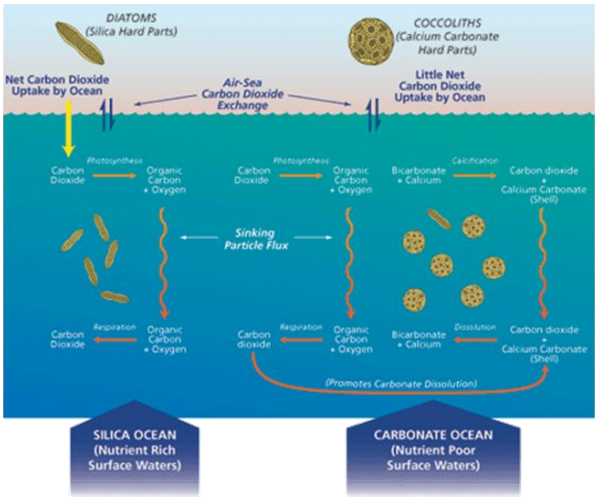

Figure 1.2. Ocean carbon cycle processes (modified from Honjo [1997]).

The historical approach for quantifying ocean primary production was to develop algorithms based on chlorophyll concentrations (Chl), such as that introduced by *Behrenfeld and Falkowski* [1997]. Their algorithm also incorporated sea surface temperature (SST) and photosynthetically-available radiation (PAR), both of which are available with high accuracy from satellite observations. A problem with deriving chlorophyll concentrations using ocean color is that other in-water constituents also absorb blue light, particularly colored dissolved organic matter (CDOM), and are ubiquitous in the surface ocean [*Siegel et al.*, 2005]. The chlorophyll-a absorption peak is at 443 nm, but CDOM absorption continues to increase at shorter wavelengths. The CZCS did not have any bands in the near-UV which would have allowed for the separation of these pigments. SeaWiFS, MODIS, and other "second generation" sensors have incorporated a band at 412 nm that allows the retrieval of CDOM [see *Siegel et al.*, 2005]. The impact of this uncertainty is illustrated in Figure 1.3, which compares primary production estimates using the standard NASA chlorophyll algorithm (which does not account for spatio-temporal variability in CDOM) and chlorophyll derived from a reflectance inversion algorithm [*Maritorena et al.*, 2002] that resolves CDOM variability. The difference in global annual production for these two chlorophyll estimates is roughly 16 GtC/yr, **representing an uncertainty in annual ocean productivity of ~30%!** *Constraining this uncertainty requires extension of measurement bands into the near-ultraviolet (to reduce uncertainties in CDOM retrievals) and improved spectral resolution in the visible band to improve quantification of phytoplankton pigment absorption.*

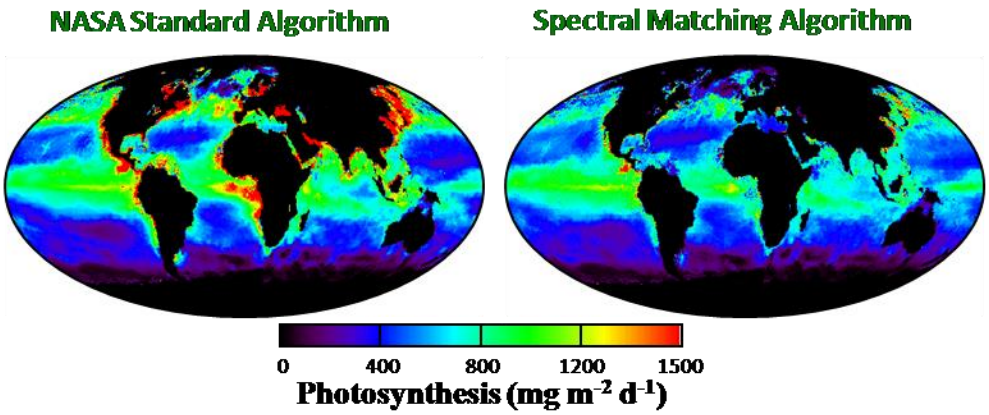

Figure 1.3. Net primary production as computed using chlorophyll-a derived from two different algorithms, the NASA empirical radiance ratio algorithm and a reflectance inversion algorithm (also called spectral matching).

In addition to the challenge of accurately retrieving surface phytoplankton pigment concentrations, current net primary production (NPP) algorithms do not accurately account for phytoplankton physiological variability. Specifically, the concentration of phytoplankton pigments is a function of both the standing stock of phytoplankton (biomass) and their physiological state (which impacts intracellular pigment levels). **Without distinguishing these two sources of variability, accurate estimates of NPP cannot be made and consequently, neither can accurate estimates of change over time**. For example, if a decrease in surface chlorophyll is observed with increasing surface temperature (as found over the SeaWiFS record), the change could be associated with a decrease in NPP from decreasing stocks or growth rates or it could be associated with improved upper ocean light conditions (photoacclimation) that is may be paralleled by no change or even an increase in NPP. One more recent approach for addressing these issues in remote sensing data was described by *Behrenfeld et al.* [2005] and *Westberry et al.* [2008]. In their approach, coincident remote sensing retrievals of particulate backscattering coefficients and pigment absorption were used to quantify phytoplankton carbon (C) biomass and physiological state (through Chl:C ratios). While representing a significant conceptual step forward, this new approach remains compromised by inadequacies in current remote sensing and field measurement capacities. In particular, relationships between particle backscattering and phytoplankton biomass are dependent on the composition and particle size distribution of plankton ecosystems. Also, relationships between Chl:C and phytoplankton growth rates are sensitive to variations in the relative concentration of auxiliary photosynthetically active pigments. Furthermore, direct field measurements of phytoplankton C concentrations for product validation are extremely difficult and time consuming and thus are rare in historical databases. Consequently our understanding of Chl:C and its relationships with growth rate and photoacclimation are largely limited to results from laboratory experimentation. *To address these serious issues, significant expansion of the UV-VIS spectral range and resolution of remote sensing measurements are required to adequately improve estimates of particle size distributions and phytoplankton pigment absorption. To support these expanded remote sensing requirements, a significant and parallel effort is needed to establish field data sets of appropriate system properties (e.g., phytoplankton C, absorption:C ratios, growth rate, acclimation irradiance) for product validation.*

The aforementioned developments (consistent with the ACE mission design) will make major contributions toward constraining ocean productivity assessments and the accurate interpretation of observed change, but represent only a portion of the ocean carbon system. A more complete

understanding of carbon budgets requires estimates not only of carbon fixation rates but of standing stocks of carbon as well, including particulate organic carbon (POC), particulate inorganic carbon (PIC), dissolved organic carbon (DOC), and dissolved inorganic carbon (DIC). To this end, advances have already been made in developing algorithms for POC [*Gardner et al.*, 2006; *Stramski et al.*, 2008], PIC [*Balch et al.*, 2005; *Gordon et al.*, 2001], and calcification rate [*Balch et al.*, 2007] from remote sensing. Applying one such algorithm to current remote sensing data, for example, *Balch et al.* [2005]estimated the standing stocks of particulate inorganic carbon (PIC, primarily calcite) and particulate organic carbon to be 19 Mtons and 665 Mtons, respectively. *Balch et al.* [2007] further estimated the annual mean calcification rate to be 1.6 GtC/yr, which is small compared to the primary production rate, yet important for understanding changes due to ocean acidification. However, the efficiency of export of POC to PIC to the deep ocean must be factored in when considering the relative contribution to deep ocean carbon sequestration. The global determination of DOC remains elusive as DOC concentrations are not simply related to CDOM [*Nelson et al.*, 2010; *Siegel et al.*, 2002]. However regional algorithms for estimating DOC for coastal regions influenced by terrestrial inputs have been successful [e.g. *Del Castillo and Miller*, 2008; *Mannino et al.*, 2008]. Given that DOC is the largest ocean organic carbon pool, tracking the global surface concentration distribution would be a significant achievement. DIC has no optical signature and its concentrations must be modeled by knowing the fluxes in and out of the DOC pool. Estimates of air-sea CO_2 flux require ocean pCO_2 values and an algorithm for the gas transfer function. *Signorini and McClain* [2009] examined the global fluxes using the latest pCO_2 climatology [*Takahashi et al.*, 2009] with various combinations of wind products and gas transfer functions. The range of net flux values was 0.9-1.3 GtC/yr into the ocean which is somewhat less that that depicted in Figure 1.1. The expanded capabilities of the ACE ocean radiometer will result in refined estimates of surface carbon pools (e.g., PIC, POC) and rates (e.g., NPP) which can be assimilated into global models to constrain the model estimates of carbon cycling in the water column and improve estimates of surface CO_2 fluxes and carbon export to the deep ocean.

Marine Ecosystems

The world's oceans represent a mosaic of unique biomes and biogeochemical provinces. *Longhurst* [1998] identified 56 pelagic provinces based on an examination of the seasonal cycles of phytoplankton production and zooplankton consumption. While species composition can be diverse often a specific phytoplankton species or functional type dominates. There are different ways of delineating these, e.g., size class (picoplankton, nanoplankton, etc.) and functional groups (diatoms, coccolithophores, *Trichodesmium*, cyanobacteria, etc.). For instance in the subpolar North Atlantic, production early in the year is due primarily to diatoms, but later in the summer, coccolithophores become abundant, preferring more stratified conditions. Thus, depending on the physical environment, availability of macro- and micro-nutrients, illumination, and the concentration of grazers, phytoplankton populations vary in their biomass, species composition, photosynthetic efficiency, etc. These variations regulate primary production and, therefore, higher trophic levels within the ecosystem, and play an important role in the cycling of macro- and micro-nutrient concentrations. Identifying these distributions and properties and how they change on seasonal and interannual time scales is key to understanding how ecosystems function and how they respond to changes in the physical environment, whether natural or human-induced.

Until recently, research on optical identification of specific species has focused on coccolithophores and *Trichodesmium* because of their rather unique spectral reflectance signatures. Coccolithophores are made of calcite platelets and can be identified in satellite data because, at high concentrations, the reflectance is uniformly elevated across the spectrum. Global coccolithophore

distributions were first assessed using CZCS data [*Brown and Yoder*, 1994]. As discussed above, calcite can now be estimated from satellites and serves as an indicator of coccolithophore populations. However, it is not an accurate indicator of viable coccolithophore cell concentrations because much of the calcite is in the form of detached platelets. Coccolithophores prefer stratified conditions and are susceptible to acidification. Thus, tracking calcite spatial distributions and concentrations over time will be a focus of future ecosystem research as it relates to climate change. While this work may not require additional spectral coverage in the future, it does require accurate sensor calibration and stability monitoring.

Another phytoplankton genus with a distinctive spectral signature is *Trichodesmium*, a cyanobacterium. *Trichodesmium* have gas-filled vacuoles or trichomes, elevated specific absorption coefficients below 443 nm, and uniformly high particle backscatter coefficients in the visible spectrum. *Trichodesmium* is nitrogen-fixing and can bloom in areas of low ambient nitrate. *Westberry et al.* [2005] found that if the concentration of trichomes is sufficiently high (3200 L^{-1}), detection by SeaWiFS is possible (and a sensor with greater SNRs could potentially detect lower concentrations). *Westberry and Siegel* [2006] mapped the global distribution of *Trichodesium*, which was consistent with global geochemical inferences made by *Deutsch et al.* [2007], and estimated that the blooms fix 60 TgN/yr which is a four- to six-fold increase over estimates of just 20 years ago [*Schlesinger*, 1997]. Based on the specific absorption spectrum, satellite observations below 412 nm should help improve quantification of *Trichodesium* concentrations.

Going beyond coccolithophores and *Trichodesium* requires the separation of functional groups with different pigment compositions and, therefore, subtle differences in reflectance spectra. Given the limited number of spectral bands that heritage sensors have, separation is a challenge and the uncertainties in the distributions must be high and are difficult to verify because only crude climatologies of species distributions are available. used *in situ* databases of reflectance, pigments, functional groups and SeaWiFS reflectances to estimate global open ocean distributions of haptophytes, *Prochlorococcus*, *Synechococcus*-like cyanobacteria (SLC), and diatoms. However, the number of phytoplankton species or size classes that can be estimated is currently limited by the number of SeaWiFS spectral bands.

Enhancing the spectral resolution and spectral range of ocean color measurements can greatly enhance retrieved information on plankton composition. The approach for using such information is referred to as "spectral derivative analysis" and has been demonstrated at 'ground level' by multiple investigators. For example, *Lee et al.* [2007a] used 400 hyperspectral (3 nm resolution) reflectance spectra from coastal and open ocean waters to examine taxonomic signatures in the first- and second-order derivatives. Their analysis indicated very pronounced peaks representing slight spectral inflections due to varying pigment absorption and backscatter characteristics of the water samples. An alternative approach (differential optical absorption spectroscopy) was used by *Vountas et al.* [2007] and *Bracher et al.* [2009], and applied to hyperspectral Scanning Imaging Absorption SpectroMeter for Atmospheric CHartographY (SCIAMACHY) imagery (0.2-1.5 nm resolution) to derive global distributions of cyanobacteria and diatoms. These studies show that realistic distributions of functional groups can be extracted from satellite data and underscore the requirement for the ACE ocean radiometer to provide hyperspectral data from the UV to the NIR.

In addition to retrieving information on phytoplankton composition through analyses of spectral absorption features, studies have also been conducted on remotely characterizing particle size distributions of natural plankton assemblages. Retrieved particle size distributions provide insight on relationships between scattering coefficients and total particulate organic carbon, as well as the relative contribution of various phytoplankton size classes to bulk standing stocks. Most recently, *Kostadinov et al.* [2009] extended the work by *Loisel et al.* [2006] on spectral particle backscatter coefficient to derive

global distributions of dominant phytoplankton size classes contributing to total biomass [Figure 1.4]. Here again, higher spectral range and resolution than heritage ocean color bands will significantly improve retrieved properties.

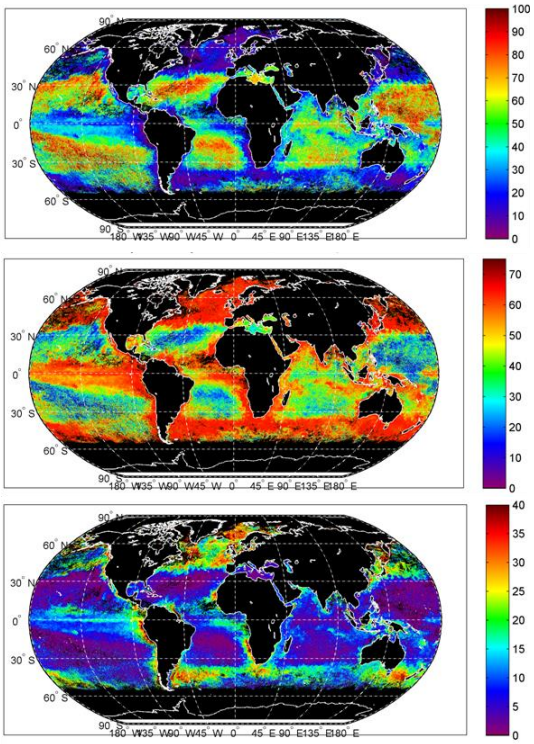

Figure 1.4. Global distributions of three particle size classes (modified from Konstadinov et al. [2009]).

Phytoplankton Physiology

Phytoplankton acclimate to environmental conditions (e.g., nutrients, temperature, and light) on time scales from seconds to seasons. These physiological adjustments influence their absorption spectra, growth rates, C:chl ratios and other characteristics. Intracellular changes in chlorophyll concentration in response to variations in mixed layer light levels alone can span over one order of magnitude, and significantly influence our ability to accurately interpret the satellite chlorophyll record and its relationship to predictions of NPP (see above). *Behrenfeld et al.* [2008] demonstrated phytoplankton physiological variability was quantified from remote sensing ratios of absorption and scattering properties and provides an illustration of the magnitude of this effect. However, accurate estimation of physiological variability requires increased spectral information.

In addition to light effects on phytoplankton acclimation states, the *degree of nutrient stress* (mild, severe) and the *type of nutrient stress* (e.g., Nitrate, Phosphate, Iron (Fe)) contribute a physiological signature to remotely derived pigment fields and will certainly be influenced by changing climate forcings on upper ocean ecosystems. One nutrient stress of particular interest is that of iron limitation. The role of iron as a major factor limiting global phytoplankton concentrations and primary production [*Martin and Fitzwater*, 1988]has been studied through a number of iron enrichment experiments and modeling studies of aeolian dust transport and deposition (see the ocean-aerosol interaction chapter). Diagnostic indicators of iron stress have also been developed for field deployments, including expression of the photosynthetic electron acceptor, flavodoxin, which replaces ferridoxin under low iron conditions [*LaRoche et al.*, 1996], and unique fluorescence properties of the oxygen-evolving photosystem II complex associated with iron stress [*Behrenfeld and Boss*, 2006]. From this field-based fluorescence study, Behrenfeld et al. (2006) predicted that satellite fluorescence measurements may provide a means for assessing global distributions of iron stress. In a subsequent study, *Behrenfeld et al.* [2009]used MODIS fluorescence line height (FLH) data to calculate global fluorescence quantum yields (ϕ), corrected for effects of pigment packaging and non-photochemical quenching, and demonstrated a strong correspondence between elevated ϕ values, low aeolian dust deposition, and model [*Moore and Braucher*, 2008; *Moore et al.*, 2006; *Wiggert et al.*, 2006] predictions of iron limited growth [Figure 1.5]. These studies further demonstrate the potential for

extracting basic information on ecosystem properties far beyond simply measuring chlorophyll-a and are significant design drivers for ACE.

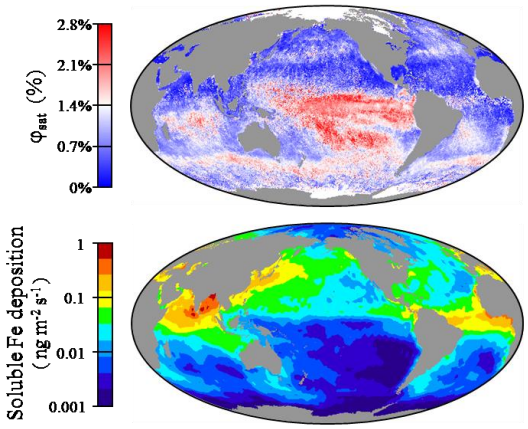

Figure 1.5. Chlorophyll fluorescence yield (top) as an indicator of soluble iron deposition (bottom; model). Modified from Behrenfeld et al. [2009].

Near-shore and Estuarine Processes

Unlike the SeaWiFS and MODIS (sensors designed for open ocean scientific objectives), the ACE science objectives also involve optically complex ocean margins, the land-sea interface, and larger estuarine systems, and must be capable of supporting coastal management and environmental monitoring requirements as well. These areas form the interface between the terrestrial and open ocean provinces and are the sites of very high primary production rates and biogeochemical transformations of carbon, nitrogen, and phosphorous. These processes are particularly important where freshwater discharge from major terrestrial drainage basins and or/population centers are focused, e.g., Mississippi River delta, Chesapeake Bay, San Francisco Bay, Gulf of Maine, Pamlico Sound, and Pudget Sound. There is considerable debate within the science community as to what fraction of global marine primary production and carbon sequestration actually occurs in these areas and adjacent continental shelves and the "continental shelf pump" [*Muller-Karger et al.*, 2005; *Tsunogai et al.*, 1999; *Yool and Fasham*, 2001]. *Muller-Karger et al.* [2005] estimated that the continental margins account for more than 40% of the global ocean carbon sequestration. However, satellite primary production algorithms do not work in many continental shelf and shallow water regions like the U.S. southeast shelf [*Signorini et al.*, 2005]. Deriving more accurate estimates of primary production and related quantities in complex coastal regions is a primary ACE science objective.

Other ACE requirements are associated with water quality and red tides. Eutrophication, a depletion of water column oxygen due to the decay of high concentrations organic matter often resulting from enhanced agricultural/sewage runoff nutrient loads, is a serious problem in many coastal regions. The Mississippi River outflow hypoxic or "dead zone" is one highly publicized example [*Goolsby*, 2000]. This condition has a significant impact on ecosystem health, commercial fisheries, and even tourism. In some cases like the Baltic Sea, the events are linked to surface blooms of nitrogen-fixing cyanobacteria which can be detected from satellite [*Kahru et al.*, 2007]. In other cases, like the U.S. Gulf coast, there is no strong correlation between surface chlorophyll and hypoxia [*Walker and Rabalais*, 2006] in which case a sensor more capable than the present day instruments may facilitate new detection approaches. While not necessarily related to eutrophication, harmful algal blooms (HABs) also affect fisheries and are a threat to public health. *Kahru and Mitchell* [1998] showed that spectral coverage between 340-400 nm is necessary for detecting red tides and more recent studies have focused on utilizing the MERIS 710 nm band [*Gower et al.*, 2005]. SeaWiFS and MODIS do not have these wavelengths. Groups within NOAA responsible for red tide monitoring are currently using MERIS data to refine detection algorithms [*Wynne et al.*, 2008]. The ACE ocean radiometer should provide capabilities needed to support the most advanced HAB detection algorithms.

In these waters, pigment and particulate complexes are more diverse and concentrated making the spectral reflectances more varied [e.g. *IOCCG*, 2000]. As a result, the spectra are amplified in the red

portion of the spectrum and depressed in the UV and blue. Heritage sensors did not exploit applications in the green and red portions of the spectrum. In fact, some MODIS ocean bands saturate in turbid waters, so care must be taken in specifying saturation radiances. Bands in the near-infrared (NIR) were designed for aerosol corrections. However, turbid waters have finite reflectances in the NIR that compromise the aerosol correction resulting in over-corrections. Over the past decade, a number of algorithms to remove or avoid this problem have been developed, e.g.,*Siegel et al.* [2000] using NIR bands, and *Wang and Shi* [2005] using MODIS shortwave infrared (SWIR) bands. For the 2009 SeaWiFS reprocessing, the latest NIR-based aerosol correction scheme resulted in significant improvement in derived product data quality in areas like the Chesapeake Bay [*Bailey et al.*, 2010; *Werdell et al.*, 2010]. As *Werdell et al.* [2010] point out, the MODIS SWIR bands do not have adequate signal-to-noise ratios (SNR) to do the turbid water aerosol correction well. For ACE, SWIR bands with adequate SNRs will be required (see the appendix). Also, the aerosols in many coastal regions absorb radiation, and current algorithms do not handle these corrections. ACE ocean radiometer observations in the near-UV, polarization measurements from the ACE polarimeter, and aerosol height measurements from the ACE lidar coupled with improved aerosol models will greatly improve ocean color retrievals in the complex atmosphere situations.

Over the past few years, the NASA Ocean Biology and Biogeochemistry program (OBBP) recognized the need for expanding its science objectives into near-shore and estuarine waters and has supported this new emphasis through research solicitations, in situ instrumentation development, incorporation of high spatial resolution data from MODIS (250 and 500 m bands) and MERIS (300 m) into the SeaWiFS Data Analysis System (SeaDAS) software (NASA freeware developed and distributed by the NASA Ocean Biology Processing Group at Goddard Space Flight Center), etc. This research and development needs to continue to further lay the foundations for the ACE mission.

Physical-Biological Interactions

There are many ways in which physical processes influence biological processes. These include not only ocean dynamical processes like coastal and equatorial upwelling, vertical mixing due to physical stirring and buoyancy effects, ocean frontal circulation, horizontal advection, etc., but also meteorological conditions such as cloud cover, surface winds, aeolian transport and deposition of dustborne nutrients (iron), etc. These processes modulate the flux of nutrients into the euphotic zone and illumination, which together regulate photosynthesis and other geochemical reactions. Most of these processes have been incorporated into coupled circulation-biogeochemical models either on regional or global scales. There is a huge published literature (theoretical, observational, and model-based) on these topics, particularly on physical forcing of biogeochemistry. However, until recently, the feedbacks of biogeochemistry on ocean dynamics have not been considered or were thought to be of secondary importance. Also, many of the biogeochemical feedbacks are linked to aerosol and cloud properties and are discussed in the ocean-aerosol interaction chapter of this document

Biogeochemical feedbacks on ocean circulation are principally effects associated with radiation absorption near the surface that affects stratification, sea surface temperature, and air-sea heat exchange. Some early studies using satellite ocean color data highlighted “penetration radiance” [*Lewis et al.*, 1990; *Ohlmann et al.*, 1996] which is the radiance that penetrated through the mixed layer and is, therefore, not available to the coupled ocean-atmosphere system. The penetration of visible light is mostly determined by phytoplankton pigment concentrations, dissolved constituents, and particle concentrations. In low concentration waters like the western Pacific warm pool where the mixed layer is shallow, this radiant flux can be 10-15% of the incident solar irradiance [*Ohlmann et al.*, 1996; *Siegel et al.*, 1995]. In areas where pigment concentrations are high, more sunlight is absorbed near the surface resulting in warmer

temperatures. A consequence of sunlight absorption by phytoplankton is a global amplification of the seasonal cycle of SST [*Frouin et al.*, 2000]. The related changes in surface layer temperature and stratification modify surface circulation and SST patterns at levels substantial enough to impact atmospheric circulation, particularly in the tropics [*Murtugudde et al.*, 2002; *Shell et al.*, 2003].

Science Questions and Objectives

To summarize, the science objectives of the ocean biogeochemistry community have expanded remarkably over the past twenty years. This progress has been greatly facilitated by data sets from SeaWiFS and MODIS, advances in marine optics (theoretical and experimental), and a growing concern about the impacts of climate change on marine ecosystems. These new objectives require much more robust measurement systems (see text below for details), especially in terms of spectral coverage. From the discussion above, the following set of ocean science questions are being posed for the ACE mission.

- ***SQ-1:*** What are the standing stocks, composition, & productivity of ocean ecosystems? How and why are they changing?
- ***SQ-2:*** How and why are ocean biogeochemical cycles changing? How do they influence the Earth system?
- ***SQ-3:*** What are the material exchanges between land & ocean? How do they influence coastal ecosystems, biogeochemistry & habitats? How are they changing?
- ***SQ-4:*** How do aerosols & clouds influence ocean ecosystems & biogeochemical cycles? How do ocean biological & photochemical processes affect the atmosphere and Earth system? These questions link directly to Question 4 of the Ocean-Aerosol Interactions element of the ACE program.
- ***SQ-5:*** How do physical ocean processes affect ocean ecosystems & biogeochemistry? How do ocean biological processes influence ocean physics?
- ***SQ-6:*** What is the distribution of algal blooms and their relation to harmful algal and eutrophication events? How are these events changing?

These questions are directly related to the objectives of the NASA Ocean Biology and Biogeochemistry Program as outlined in its long-term planning document, *The Earth's Living Ocean, The Unseen World* [NASA OBB Working Group, 2007].

The Human-Ocean Relationship and Societal Benefits

For Earth's entire history, only one life form has ever existed with the capacity to intentionally modify the role of ecosystems on the global environment: *humans*. We are the ultimate caretakers of this planet and it is upon our shoulders that the well-being of the biosphere rests. Our recognition of this responsibility, however, is recent – emphasized by escalating impacts of an ever-growing human population. In addition, and despite a long history of technological advancement, we remain intimately dependent on the biosphere's highly interlaced food webs for our well being. Complex ocean ecosystems provide habitat and natural resources that nurture biodiversity, interact with geochemical and physical systems in the cycling of carbon and other elements, and play an essential role in the regulation of climate over annual to geologic time scales that contributes importantly to the habitability of our planet. At the same time, ocean ecosystems are fragile and highly susceptible to environmental change. One must only look at the mass extinction events in Earth's history to fully appreciate the delicate balance of species diversity and

ecosystem resilience and to understand its dependence on stability in climate and biological conditions. Today, threats to ocean ecosystems come not only from natural sources, but from human activities as well, with the human component becoming ever more prominent and well documented. As caretakers of this unique living planet, we are charged with the responsibility of understanding causes and effects of global change and protecting the diversity and invaluable services that the global oceans provide.

Understanding functional relationships within the living ocean, along with ocean-land-atmosphere feedbacks, represents a major challenge to the science community and one to which the ACE mission is particularly well poised to contribute greatly. Through its advanced observation sensor suite, this mission will allow better description and prediction of Earth system mechanisms affected by natural and anthropogenic climate changes, and assessment of how these processes feedback on the overall Earth system over time. At the same time, the ACE mission will provide a more diverse set of capabilities and data products of higher quality in coastal regions than current sensors, e.g., harmful algal bloom detection, suspended sediment concentrations, and carbon pools. The improved understanding and measurement capabilities will enable informed national policy, improved resource management practices, and decreased threats to our economy, health, safety, and national security.

1.2. Approach

Addressing the key outstanding science questions for ocean ecosystems requires significant advances in remote sensing capabilities beyond heritage sensors, improvements in strategies to remove contamination of ocean color signals by the atmosphere, and well-developed field- and on-orbit calibration and validation approaches. With the suite of ACE sensors and their advanced capabilities, more accurate- and a broader set of key ecosystem properties can be characterized globally on weekly to shorter time scales. Some of these properties are essential for answering all of the science questions outlined above, while others are targeted toward advancing understanding of a particular science issue. In some cases, the observational data largely functions to inform an overarching model, but in all cases the required set of retrieved properties creates the link between the ***Science Questions*** and ***Measurement and Mission Requirements***.

SQ-1 (Ocean Ecosystems) Approach: Quantify phytoplankton biomass, pigments, and optical properties, assess key phytoplankton groups (e.g., calcifiers, nitrogen fixers, carbon export), and estimate particle size distribution and productivity using bio-optical modeling, chlorophyll fluorescence, and ancillary data on ocean physical properties (e.g., SST, MLD, etc.). Validate these retrievals from pelagic to nearshore environments.

SQ-2 (Ocean Biogeochemical Cycles) Approach: Retrieve phytoplankton biomass and functional groups, POC, PIC, DOC, PSD and productivity from remotely sensed ocean properties. Validate these retrievals from pelagic to nearshore environments. Assimilate ACE observations in ocean biogeochemical models to provide fields for missing observations (cf., air-sea CO_2 fluxes, export, pH, etc.).

SQ-3 (Land-Ocean Interactions) Approach: Quantify particle abundance, dissolved material concentrations and their physical and optical properties. Validate these retrievals from coastal to estuarine environments. Compare ACE observables with ground-based and model-based land-ocean exchange in the coastal zone, physical properties (e.g., winds, SST, SSH, etc), and circulation (ML dynamics, horizontal divergence, etc).

SQ-4 (Atmosphere-Ocean Interactions) Approach: Quantify ocean photobiochemical and photobiological processes and atmospheric aerosol loads and distributions. Combine ACE ocean and

atmosphere observations with models and other remotely retrieved fields (e.g. temperature and wind speed) to evaluate (1) air-sea exchange of particulates, dissolved materials, and gases and (2) impacts on aerosol and cloud properties. Conduct field sea-truth measurements and modeling to validate retrievals from the pelagic to near-shore environments.

SQ-5 (Bio-physical Interactions) Approach): Compare ACE ocean observations with measurements of physical ocean properties (winds, SST, SSH, OOI assets, etc.) and model-derived physical fields (ML dynamics, horizontal divergence, etc.). Estimate ocean radiant heating and assess feedbacks. Validate from pelagic to nearshore environments.

SQ-6 (Algal Blooms and Consequences) Approach): Measure key phytoplankton biomass, pigments and key group abundance including harmful algae. Quantify bloom magnitudes, durations, and distributions, assess inter-seasonal and inter-annual variations, and compare variability to changing environmental/physical properties. Validate these retrievals from pelagic to nearshore environments.

1.3. Measurement & Mission Requirements

SeaWiFS and MODIS ocean requirements were defined in the 1980s with an emphasis on global open ocean observations of chlorophyll-a. Both sensors addressed major deficiencies in the proof-of-concept CZCS design and calibration/validation programs, e.g., the addition of NIR bands for atmospheric correction and mission-long on-orbit and field calibration measurements. Since then, the ocean optics and marine biology communities have developed capabilities and applications that far exceed the spectral coverage of these sensors and experience using these sensors has provided many "lessons learned". Also, development of climate data records requires consistent sets of spectral bands and stringent mission-long stability specifications. Together, this cumulative experience has highlighted a number of new requirements, including the following enhancements which are incorporated into the ACE ocean measurement requirements. A table is provided in the appendix below that lists 26 discrete bands and specific applications of each. Note that the table includes the SeaWiFS and MODIS bands for continuity.

1. Major advances in global ocean biological studies have been realized through the development of spectral inversion algorithms. These algorithms allow the simultaneous and mutually consistent retrieval of multiple in-water properties, including phytoplankton absorption, absorption by colored dissolved organic material, and particulate backscattering coefficients. SeaWiFS and MODIS do not provide adequate spectral coverage for optimizing the inversions. Requirement: 19 bands at specific center wavelengths between 360-748 nm characteristic of key constituent absorption and scattering features. (**Related Science – *SQ-1, SQ-2, SQ-4, SQ-5, SQ-6***)

2. The addition of a 412 nm band into SeaWiFS and MODIS has provided a first look at the separation of chlorophyll-a and CDOM using satellite ocean color imagery. Within the UV, CDOM dominates light absorption for nearly all natural waters and improvements in separation between chlorophyll-a and CDOM will occur from including measurements of water-leaving radiance in the UV. Requirement: additional bands at 360 and 380 nm. (**Related Science – *SQ-1, SQ-2, SQ-3, SQ-4***)

3. Uncertainties in current inversion retrievals by passive sensors can be reduced through simultaneous and independent measurements of particle scattering using active sensors. Recent analyses of CALIPSO data have demonstrated that space-based lidar systems can provide active measurements of subsurface scattering and possibly information on vertical distributions of particles. Requirement: Lidar measurements with parallel and perpendicular retrievals at an

ocean-penetrating wavelength and with a vertical resolution of 2 meters subsurface. (**Related Science – *SQ-1, SQ-2, SQ-3, SQ-6***)

4. Recent research has shown that phytoplankton fluorescence quantum efficiency can be derived from MODIS fluorescence data and that the quantum efficiency is related to iron limitation or stress. Requirement: Fluorescence line height bands consistent with the MODIS fluorescence line height bands for time series continuity. (**Related Science – *SQ-1, SQ-2, SQ-5, SQ-6***)

5. The research community has also explored the identification of phytoplankton functional groups using SeaWiFS and MODIS, but with high uncertainties. Recent analyses using hyperspectral SCIAMACHY on Envisat have demonstrated the promise of spectral derivative analyses. Requirement: 5 nm resolution data from 360 to 755 nm. (**Related Science – *SQ-1, SQ-2, SQ-6***)

6. Studies in optically-complex coastal waters have identified limitations in the use of blue and green bands for quantifying chlorophyll. Requirement: Additional bands in the red, and near-infrared, including 700-750 nm range, are necessary. (**Related Science – *SQ-3, SQ-6***)

7. Accurate satellite retrievals of water leaving radiances require robust and accurate corrections for atmospheric contributions to top-of-atmosphere (TOA) radiances. In short, the ocean color problem is one of low 'signal to noise', as greater than 90% of TOA radiances can be from the overlying atmosphere. In some circumstances (e.g., presence of Asian or African dust) current atmospheric corrections suffer from inadequate information on these aerosol optical properties and their vertical distribution. Requirement: Lidar 'curtain' measurement of aerosol distributions with 0.5 km vertical resolution and polarimeter broad spatial coverage to retrieve aerosol heights and single scatter albedo. Include UV bands (Item 2 above) to assist in the detection and atmospheric correction of absorbing aerosols. (**Related Science – *All SQ's***)

8. Certain required bio-optical bands overlay water vapor absorption features making corrections necessary. Requirement: Include an 820 nm band to quantify water vapor concentration. (**Related Science – *SQ-1, SQ-4,SQ-6***)

9. Programmatic research objectives oriented towards turbid coastal waters must address finite reflectances in the NIR bands which compromise the aerosol correction. Requirement: SWIR bands at 1245, 1640, and 2135 nm with substantially higher SNRs than the equivalent MODIS bands. (**Related Science – *SQ-3, SQ-6***)

10. The direct lunar calibration (Earth-viewing optics only) and in situ vicarious calibration of SeaWiFS, in particular, successfully demonstrated the climate quality ocean biology data sets necessitate highly accurate independent temporal stability monitoring (0.1% stability knowledge over the duration of the mission) and gain adjustments, respectively. The vicarious calibration required a multi-year time optical mooring deployment to establish stable gain factors. Requirement: Monthly lunar views at a fixed 7° lunar phase angle and at least one long-term vicarious calibration time series. (**Related Science – *All SQ's***)

11. Concurrency of global data products is required to address many of the ACE Ocean Ecosystems science questions and for ocean color data processing. These observations include SST, SSH, vector winds, MLD, precipitation, and O_3 and NO_2 concentrations. Requirement: Concurrency of operational satellite data and model output products. (**Related Science – *All SQ's***)

Other sensor requirements address sun-glint avoidance (sensor tilting), polarization sensitivity, SNRs, image quality (straylight, stripping, crosstalk), 2-day global coverage frequency, data quantization, and saturation radiances. To achieve the radiometric accuracy requirements of the inversion algorithms, well-developed and tested technologies and methodologies for prelaunch sensor characterization must be established in advance of flight unit testing. When all the requirements for passive ocean radiometry are tallied, the comparison with heritage sensors is striking, particularly with respect to spectral coverage [Figure 1.6].

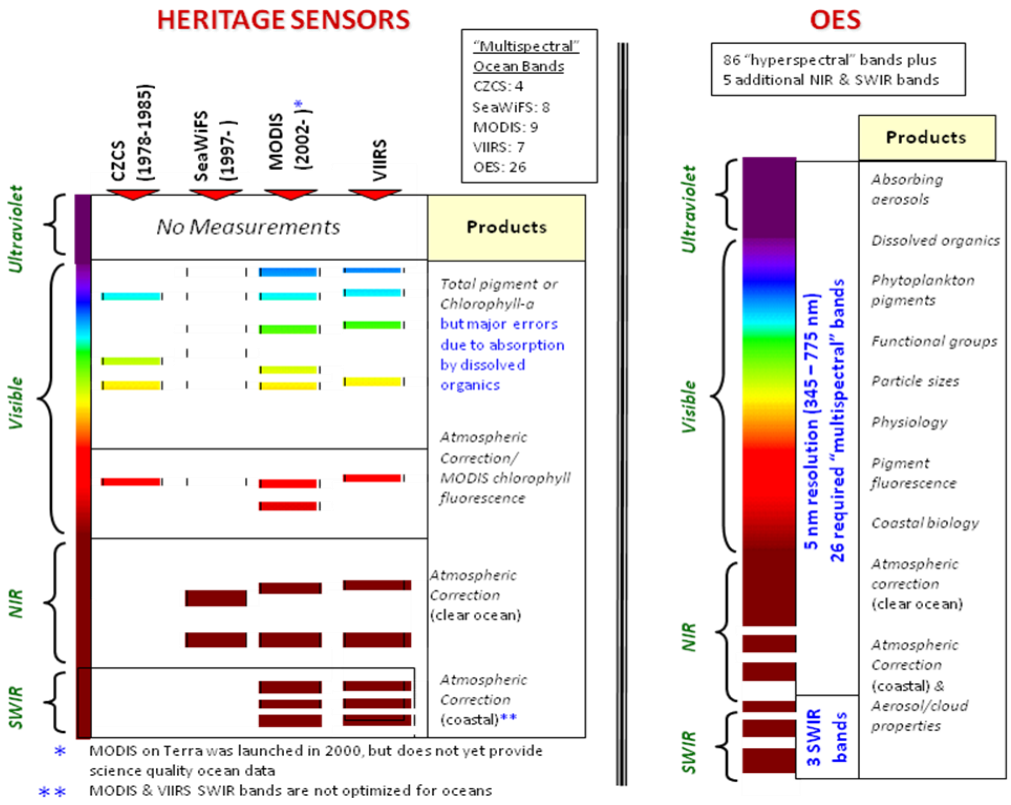

Figure 1.6. Comparison of spectral coverage of heritage sensors and the OES.

1.4. Calibration, Validation, and Observations in the Field

Observations made *in situ* are an essential and integral part of the ACE mission. Field work will consist of observations useful for calibration and validation (e.g. measurements of optical properties), but will also include measurements essential to answering the science questions that are not possible from the ACE spacecraft-based instruments. An example of these sorts of observations would be measurements of export flux (***SQ-2***) which occurs below the surface layer of the ocean and is thus not directly observable by remote sensing. Field observations will also be critical in the prelaunch phase for the purpose of developing algorithms or identifying proxy measurements that will employ the new capabilities of the ACE spaceborne instruments. Previous experience with SeaWiFS, MODIS, and related ocean color radiometers indicates that continuous assessment of calibration and validation of products, combined with periodic reprocessing of complete mission data sets, is necessary throughout the lifetime of the mission. Sustained mission-lifetime measurements will take place at selected time series sites for purposes of vicarious calibration (mission requirement 8) and product validation, and these will be augmented by measurements made on cruises and moorings of opportunity, and in intensive field campaigns. Product

validation and algorithm development will be facilitated by the continuation of the NASA SeaBASS database, which stores bio-optical (and now biogeochemical) data collected concurrently with satellite overpasses.

Science Discipline	Field Parameter	Analytical Levels CP	RM	UB	PM	TR	Deployment Tech. M	T	G	R	A	S	Ocean Ecosystems Science Questions 1	2	3	4	5	6
Optical	Radiometry											C	1	2	3	4	5	6
	Oceanic IOPs										?		1	2	3	4		
	Atm. Optical Properties													2		4	5	
Carbon Cycle	CDOM											C		2	3	4	5	
	DOC											C		2	3	4		
	POC											C	1	2	3	4		
	PIC											C	1	2	3	4		
	Vertical Flux			?									1	2		4		6
	TSM													2	3	4		
Nitrogen Cycle	PON												1	2	3	4		
	Ammonium		?			?								2	3	4		6
	Nitrate/Nitrite		?			?			?				1	2	3	4		
Biological	PP											C	1	2		4	5	6
	HPLC pigments											C	1	2		4		6
	Natural fluorescence											C	1	2				6
	MAAs												1					6
	Micro Taxonomy			?									1	2		4		6
	Pico Taxonomy			?									1	2		4		6
	O2		?											2			5	6
Physical	Salinity					?						C			3	4	5	6
	Temperature											C	1		3	4	5	6
	Surface meteorology		?										1			4	5	6
	Particle size/abundance		?								?		1		3	4		
Chemical	DMS, DMSp												1	2		4		
	Silicate		?			?							1	2	3	4		
	Phosphate		?			?							1	2	3	4		6
	pCO2		?													4		
	Trace nutrients		?										1	2		4	5	
	pH	?	?											2		4		

Most stringent requirements are for validation of satellite climate data records (CDR, C)

Moor. Tower Glider R/V A/C Sat.

Key to Analytical Levels

CP: Community protocols (experimental method)
RM: Reference materials (research)
UB: Uncertainty budget (semi-quantitative)
PM: Performance metrics (quantitative)
TR: NIST (or other) traceability (CDR)

Readiness Capabilities for Analytical Levels and Deployment Technologies

Little capability demonstrated, significant work to be done.
Some capability demonstrated, but more work needs to be done.
Mature capability (calibration and validation quality).

Figure 1.7. Ocean in situ/laboratory measurements requirements. The "?" implies the status is not known.

New sensor capabilities will require corresponding capabilities in the field. A road map for technology development is being developed by the community that describes necessary advancements required to make best use of the future ACE sensor suite in solving the science questions laid out by the ACE Ecosystems working group. Figure 1.7 shows the current state of the art for a list of parameters that are required for particular SQs, in terms of analytical capability and deployment technology. For the ACE mission this includes biogeochemical parameters in addition to the traditionally measured radiometric quantities. Pressing needs here include extension of currently measured radiometric and inherent optical properties into the UV and further into the NIR.

Intensive field campaigns will be designed to address particular interdisciplinary questions with shipborne measurements complementing the ACE sensor suite. Specific proposed cruises/topics are being discussed by the community now. Campaigns will be designed to take maximum advantage of suborbital resources (e.g. airborne and shipborne measurements) to make best use of the available remote sensing data. Topics will include ocean-aerosol interactions in coastal and open-ocean areas where atmospheric correction due to dust and other terrestrial aerosols has been challenging for current sensor technology.

One strategy for efficiently pursuing ACE goals in interdisciplinary field campaigns is to cooperate with national and international coordinating groups who are proposing large field programs. Examples of these include OCB (Ocean Carbon and Biogeochemistry, http://www.us-ocb.org/), addressing ***SQ-1*** & ***SQ-2***; SOLAS (Surface Ocean-Lower Atmosphere Study, http://www.us-solas.org/), addressing ***SQ-4***; and CLIVAR/Carbon Repeat Hydrography Project (http://ushydro.ucsd.edu/), addressing ***SQ-2*** & ***SQ-5***.

The ACE Ocean Working Group includes those who participated in ocean related activities such as defining the ocean science objectives and questions, performed sensitivity analyses, provided ocean parameter measurement specifications, participated in routine teleconferences, attended ACE meetings, assisted in sensor and mission concept studies, and other deliberations reflected in this document and appendices. This group included Z. Ahmad, B. Balch, M. Behrenfeld (co-chair), E. Boss, J. Chowdhary, C. Del Castillo, R. Frouin, S. Gasso, H. Gordon, S. Hooker, Y. Hu, T. Kostadinov, Z. Lee, A. Mannino, S. Maritorena, C. McClain (co-chair), N. Meskhidze, M. Mulholland, N. Nelson, D. Siegel, D. Stramski, R. Stumpf, M. Wang, J. Werdell, and T. Westberry. Paula Bontempi has served as the NASA Headquarters ACE ocean program scientist since the inception of the ACE mission definition activity in 2008.

Appendix to Chapter 1

ACE Ocean Ecosystems Ocean Ecosystems Sensitivity Analyses and Measurement Requirements

ACE Ocean Working Group

The appendix has four sections on remotely sensed optical, biological, and biogeochemical parameters related to the science questions, atmospheric correction sensitivity to noise, bio-optical algorithm sensitivity to noise, and a summary of ocean radiometer measurement requirements. The atmospheric correction analysis was conducted by Menghua Wang (NOAA/NESDIS) and Howard Gordon (U. of Miami). The bio-optical algorithm study was conducted by Stephane Maritorena (UC/Santa Barbara) using inputs from the Wang and Gordon study.

2.1. Remotely Sensed Ocean Optical, Biological, and Biogeochemical Parameters

Associated with each of the science questions is a set of geophysical parameters that must be measured in order to address the question. Remote sensing retrievals for each of these parameters requires an algorithm that transforms the basic water-leaving radiances or remote sensing reflectances into an estimated value of that parameter over a range of values. In Table 2.1 on the following 6 pages, the various desired geophysical parameters are shown in the left-most column. For each parameter, the second and third columns indicate baseline and threshold ranges for the parameter, respectively. Here, the 'baseline' range represents the full desired retrieval range for a given parameter and is the range of values between the 1% and 99% region for the parameter frequency distribution. The 'threshold' range is the required retrieval range for a given parameter and represents the 5% to 95% region of the frequency distribution. Baseline and threshold values for the geophysical parameters defined in Table 2.1 were based on analyses of both field and historical satellite measurements. Specific information regarding these analyses for each parameter is provided in the right-most column of comments. It should be noted that values for each parameter have been measured that exceed even the baseline range, but these values are found under extreme and rare conditions and were not viewed as critical retrieval requirements for a satellite mission focused on global ocean properties. Importantly, the range of parameter values shown in Table 2.1 places specific requirements on ACE satellite radiometry regarding spectral bands, spectral ranges, and data quality from the sensor (e.g., signal-to-noise ratio and radiometric accuracy), as well as requiring algorithm development and algorithm sensitivity analyses.

Table 2.1. ACE ocean geophysical parameters, retrieval baseline ranges, and retrieval threshold ranges. See comments in right-most column regarding data sets and other notes on parameter ranges.

Geophysical Parameter	Baseline Range	Threshold Range	Comments
Remote sensing reflectance (Rrs)	Rrs(340) 0.0015 - 0.020 sr^{-1} Rrs(380) 0.0017 - 0.020 sr^{-1} Rrs(412) 0.0011 - 0.033 sr^{-1} Rrs(443) 0.0016 - 0.024 sr^{-1} Rrs(490) 0.0023 - 0.014 sr^{-1} Rrs(510) 0.0026 - 0.011 sr^{-1} Rrs(531) 0.0021 - 0.010 sr^{-1} Rrs(547) 0.0014 - 0.009 sr^{-1} Rrs(555) 0.0014 - 0.008 sr^{-1} Rrs(670) 0.0000 - 0.002 sr^{-1} Rrs(678) 0.0000 - 0.002 sr^{-1} Rrs(683) 0.0000 - 0.012 sr^{-1}	Rrs(340) 0.0020 - 0.015 sr^{-1} Rrs(380) 0.0030 - 0.017 sr^{-1} Rrs(412) 0.0035 - 0.028 sr^{-1} Rrs(443) 0.0038 - 0.021 sr^{-1} Rrs(490) 0.0042 - 0.012 sr^{-1} Rrs(510) 0.0036 - 0.008 sr^{-1} Rrs(531) 0.0027 - 0.006 sr^{-1} Rrs(547) 0.0019 - 0.005 sr^{-1} Rrs(555) 0.0018 - 0.005 sr^{-1} Rrs(670) 0.0001 - 0.001 sr^{-1} Rrs(678) 0.0001 - 0.001 sr^{-1} Rrs(683) 0.0000 - 0.001 sr^{-1}	Ranges in the 412-678 nm region are based on the SeaWiFS and MODIS-AQUA data. Ranges at 340, 380 and 683 nm are based on field measurements from a variety of oceanic and coastal stations (n > 1,000) extracted from the NASA SeaBASS archive.
Inherent optical properties *Absorption coefficients* - total absorption (a) - phytoplankton absorption (a_{ph}) - detrital absorption (a_d) - colored dissolved organic material absorption (a_{CDOM}) *Backscatter coefficient* (bb) *Beam attenuation* (c)	 a(412) 0.020 - 2.0 m^{-1} a(443) 0.020 - 1.8 m^{-1} a(555) 0.065 - 1.5 m^{-1} a(676) 0.460 - 1.8 m^{-1} a_{ph}(443) 0.003 - 1.2 m^{-1} a_d(443) 0.0004 - 0.6 m^{-1} a_{CDOM}(443) 0.002 - 0.9 m^{-1} b_{bp}(443) 0.0003 - 0.1 m^{-1} c(412) 0.03 - 10.0 m^{-1} c(443) 0.03 - 10.0 m^{-1} c(555) 0.08 - 10.0 m^{-1}	 a(412) 0.03 - 0.8 m^{-1} a(443) 0.03 - 0.7 m^{-1} a(555) 0.08 - 0.6 m^{-1} a(676) 0.47 - 0.8 m^{-1} a_{ph}(443) 0.007 - 0.7 m^{-1} a_d(443) 0.001 - 0.3 m^{-1} a_{CDOM}(443) 0.003 - 0.5 m^{-1} b_{bp}(443) 0.001 - 0.003 m^{-1} c(412) 0.1 - 0.5 m^{-1} c(443) 0.1 - 0.5 m^{-1} c(555) 0.1 - 0.5 m^{-1}	For total a and c, 1% and 5% values were based on OSU data base (450 near surface data points), 95% values based on data from the Philippines (PHILEX, two cruises), and the 99% values based on coastal OASIS observations. The a_p, a_d, and a_{CDOM} values are based on NOMAD data (Mannino et al 2008, Nelson et al 2010). BIOSOPE data from the ultra-oligotrophic South Pacific gyre were used in assessing lower limits of baseline ranges (Huot et al., 2008; Bricaud et al., 2010). bbp(443) values are based on the GSM (Maritorena et al. 2002) and QAA (Lee et al 2002) inversion models applied to MODIS L3 data,

	c(676) 0.47 - 10.4 m^{-1}	c(676) 0.5 - 0.9 m^{-1}	in addition to a subset of field measurements available in SeaBASS. Coastal, sediment-dominated waters have values well beyond the stated maximum. a_{CDOM} values are based on field data which contain sampling bias in coastal regions. Recommended maxima based on satellite data and field measurements from high CDOM areas (coastal & river plumes) are 3 m^{-1} for threshold and 10 m^{-1} for baseline.
Diffuse attenuation coefficient for downwelling plane irradiance at 490 nm [Kd(490)]	Kd(490) 0.02 - 4.0 m^{-1}	Kd(490) 0.02 - 1.5 m^{-1}	Based on >6,100 in-water profiles, spanning the clearest waters (South Pacific gyre, Arctic ice zone) to very turbid and shallow riverine waters. Values are based on data in the near-surface extrapolation interval--they are not "bulk" values (Morel et al. 2007). Kd can also be derived for other wavelengths.
Incident Photosynthetically Available Radiation (PAR) *Instantaneous* *24-hr flux*	0 - 2,200 µmol quanta m^{-2} s^{-1} 0 - 60 mol quanta m^{-2} d^{-1}	100 - 2,100 µmol quanta m^{-2} s^{-1} 10 - 55 mol quanta m^{-2} d^{-1}	In some partly cloudy situations, the upper values for instantaneous PAR can be 10-15% higher due to reflection by the side of clouds. Ranges for 24 hr PAR data based on 2004 MODIS data corrected for cloudiness and available at: oceancolor.gsfc.nasa.gov/
1% PAR depth ($Z_{1\%}$)	10 - 150 m	35 - 135 m	Ranges are based on 2008 MODIS Rrs retrievals, with the 1%PAR depth calculated following Lee et al. (2007).

Particulate inorganic carbon concentration (PIC)	1.2 * 10^{-5} - 5.3 * 10^{-4} mol m^{-3}	1.9 * 10^{-5} - 3.3 * 10^{-4} mol m^{-3}	Values based on Atlantic Meridional Transect cruises (covering the oligotrophic gyres to eutrophic waters). N=481. Samples processed by first filtering seawater onto 0.4um polycarbonate filters and subsequently rinsed with potassium tetraborate (pH8), to rinse away seawater calcium. PIC derived from particulate calcium measurement using inductively-coupled plasma optical emission spectroscopy. Samples corrected for seawater calcium by also measuring the sodium line with the ICP-OES. Statistics calculated on log transformed data.
Particulate Organic Carbon concentration (POC)	15 - 2,000 mg m^{-3}	20 - 500 mg m^{-3}	Values based on 804 field measurements from ultra-oligotrophic to turbid coastal environments. Minimum and maximum surface values of POC derived from both field and satellite data are about 10 mg m^{-3} and 10,000 mg m^{-3}. In extreme cases values in excess of 10,000 mg m^{-3} have been observed
Dissolved Organic Carbon concentration (DOC)	35-800 µmol L^{-1}	40-500 µmol L^{-1}	Values based on field data. Surface DOC in the field ranges from 35 to 1,000 µmol L^{-1}. Typical river plume DOC is 650 umol L^{-1} for Arctic and tropical rivers, but DOC can exceed 1,000 µmol L^{-1}.
Suspended Particulate Matter concentration (SPM)	25 - 70,000 mg m^{-3}	45 - 15,000 mg m^{-3}	Values based on 271 field measurements from ultra-oligotrophic to turbid coastal

			environments. For this data set, the minimum SPM = 22 mg m^{-3} and the maximum ~140,000 mg m^{-3}. In some aquatic environments higher values can be observed.
Particle size characteristics (size ranges indicted here)	0.05 - 2,000 µm	0.8 - 200 µm	Threshold values reflect current measurement capabilities for seawater samples using electronic counting/sizing (e.g., Coulter) and laser diffraction (e.g., LISST). Baseline values represent a desired, environmentally-relevant range requiring near-term instrument/ technique development.
Total Chlorophyll-a concentration (TChl-a)	0.015 - 40 mg m^{-3}	0.030 - 25 mg m^{-3}	Values based on field and satellite (SeaWiFS) data. Field data are from SeaBASS and include HPLC and Turner fluorescence measurements.
Other phytoplankton pigments	To be defined	To be defined	
Phytoplankton Carbon concentration (C_{phyto})	0.15 - 800 mg m^{-3}	3.0 - 450 mg m^{-3}	Values based on satellite retrievals of b_{bp} converted to C_{phyto} following Westberry et al. (2008).
Normalized Fluorescence Line-height (FLH)	0.0001 - 0.025 mW cm^{-2} µm^{-1} sr^{-1}	0.001 - 0.015 mW cm^{-2} µm^{-1} sr^{-1}	Values based primarily on MODIS L3 data, but in situ data (NOMAD) were also used for evaluating maximum criteria
Fluorescence Quantum Yield (FQY)	0.0003 - 0.05 fluoresced photons (absorbed photons)$^{-1}$	0.001 - 0.02 fluoresced photons (absorbed photons)$^{-1}$	Values based on MODIS L3 data following Behrenfeld et al. (2009), which includes a correction for non-photochemical quenching that reduces FQY values at low-light

Net Primary Production (NPP)	55 - 8,500 mg m^{-2} d^{-1}	90 - 4,500 mg m^{-2} d^{-1}	Values based on field and satellite (SeaWiFS) data. Satellite data are from the VGPM (Behrenfeld & Falkowski 1997). Field data are from the OSU productivity website: www.science.oregonstate.edu/ocean.productivity/
Phytoplankton physiological properties *Chl:C* *Growth Rate*	 0.0005 - 0.3 mg mg^{-1} 0.00 - 1.9 d^{-1}	 0.001 - 0.1 mg mg^{-1} 0.01 - 1.5 d^{-1}	Growth rate values based on satellite Chl:C data, light attenuation, and mixing depth (Westberry et al. 2008).
Phytoplankton groups *Size-based groups expressed as a fraction of total algal chlorophyll*	 microphytoplankton: 0 - 0.9 nanophytoplankton: 0 - 0.9 picophytoplankton: 0 - 1.0	 microphytoplankton: 0 - 0.7 nanophytoplankton: 0.2 - 0.8 picophytoplankton: 0 - 0.8	Size-based groups from exclusively open-ocean field HPLC- pigment data (Uitz et al. 2006), with a baseline surface chlorophyll-a range of 0.03 - 5.8 mg m^{-3}. Only data from the first optical depth are included. See Uitz et al. (2006) for details. Alternative approaches for defining phytoplankton groups are also under investigation.
Trichodesmium concentration	0 – 10,000 filaments L^{-1}	0 – 5,000 filaments L^{-1}	Values based on ~20 years of field data (largely epifluorescence microscopy of filtered seawater). When necessary, filaments L^{-1} was estimated assuming 200 filaments $colony^{-1}$ (Carpenter, 1983). A large bloom can exceed 10^6 filaments L^{-1}.
Coccolith concentration	293 - 814,930 detached coccoliths mL^{-1} 34 - 3,624 plated	760 - 314,000 detached coccoliths mL^{-1} 59 - 2,066 plated	Values based on field data from Atlantic Meridional Transect cruise 17 (n=412 samples) which included oligotrophic to temperate waters and a coccolithophore bloom

	coccolithophores per coccolith aggregates mL^{-1}	coccolithophores per coccolith aggregates mL^{-1}	Statistics calculated on log transformed data. Note, highest published concentrations of detached coccoliths in the field are ~500,000 mL^{-1}. The baseline upper range of 800,000 mL^{-1} (statistically defined here by the upper 99^{th} percentile of log-normal variance), thus, appears high. Plated coccolithophores are combined with coccolith aggregates because discrimination is difficult when using birefringence microscopy.

2.2. Simulations for the NIR and SWIR SNR Requirements for Atmospheric Corrections

Atmospheric correction for ocean color product is extremely sensitive to sensor spectral band calibration errors, as well as to radiometric noise. This is due to the considerably low radiance from the ocean compared to the sensor-measured top-of-atmosphere (TOA) radiance. The sensor spectral band radiometric performance can be characterized by the signal to noise ratio (SNR). To understand the radiometric noise effects on the derived normalized water-leaving reflectance spectra, simulations of atmospheric correction, using the two near-infrared (NIR) bands (765 and 865 nm) and various combinations of the shortwave infrared (SWIR) bands (1240, 1640, and 2130 nm), have been carried out for several levels of sensor noise.

Noise Model. A Gaussian distribution (with mean value = 0) is used for the noise simulations. The standard deviation (STD) of the Gaussian distribution is the radiance noise level (i.e., related to the SNR values). The simulated reflectance noise is then added into the TOA reflectance at various NIR and SWIR bands that are used for making atmospheric correction. Eight noise levels are generated, corresponding to eight SNR values of 25, 50, 100, 200, 400, 600, 800, and 1000. It is noted that the reflectance noise is only added into the bands that are used for atmospheric correction (e.g., two NIR bands), and UV and visible bands are noise free in all simulations discussed in this subsection. The reflectance noises are spectrally incoherent.

Atmospheric Correction. Atmospheric correction simulations using two NIR bands (Gordon and Wang, 1994) and various SWIR bands [*Wang*, 2007] have been carried out including reflectance noise levels for the corresponding NIR and SWIR bands. Specifically, simulations were carried out for a typical Maritime aerosol model (M80) and a Tropospheric model (T80), where the T80 model is actually M80 model without the large size fraction, for aerosol optical thicknesses (at 865 nm) of 0.05, 0.1, 0.2, and 0.3. The M80 and T80 aerosol models were not used in the aerosol lookup tables for atmospheric correction [*Gordon and Wang*, 1994; *Wang*, 2007]. Simulations were performed for a case with solar-zenith angle of 60°, sensor-zenith angle of 45°, and relative azimuth angle of 90°.

SNR Simulations. For each case, atmospheric correction for 5000 noise realizations with a given SNR value was carried out. For example, for a case with aerosol optical thickness (AOT 865 nm of 0.1, 5000 reflectance noise samples (with a given SNR value) were generated and added into the TOA NIR (765 and 865 nm) reflectance values. The NIR atmospheric correction [*Gordon and Wang*, 1994] was then performed 5000 times to generate the corresponding normalized water-leaving reflectance spectra error. The same procedure was carried out for all four AOTs and also for the SWIR algorithm [*Wang*, 2007]. In the SWIR atmospheric correction, however, the Gaussian noise was of course added into the SWIR bands (error free for UV to NIR bands). This produces the uncertainty in the derived normalized water-leaving reflectance from the UV to the red (or NIR in the case of the SWIR bands). In effect, the simulated uncertainty includes errors from both the atmospheric correction algorithm and the added Gaussian noise in the NIR or SWIR bands. The reflectance uncertainty spectra (from UV to red) are then used for the bio-optical model sensitivity analysis by Stephane Maritorena.

Example Results. Figure 1 provides sample results in the reflectance uncertainty spectra (UV to red or UV to NIR) with simulations from atmospheric correction algorithm using the NIR or SWIR bands. The error in the normalized water-leaving reflectance, $[\rho_w(\lambda)]_N$, is actually the standard deviation of the derived uncertainty in $[\rho_w(\lambda)]_N$ over the 5000 Gaussian noise realizations, i.e., each point in the plot was derived from 5000 simulations ($[\rho_w(\lambda)]_N$ errors were first obtained with these 5000 simulations and then STD error was derived). The STD error was computed assuming that the mean value = 0 (i.e., error free).

Figures 2.1(a) and 2.1(b) are results for the NIR atmospheric correction algorithm (using 765 and 865 nm) with the M80 and T80 aerosol models, respectively, while Figures 2.1(c) and 2.1(d) are results for the M80 and T80 aerosols using the SWIR atmospheric correction algorithm (with bands of 1240 and 1640 nm) for various SNR values. Note that for the SWIR results [Figures 2.1(c) and 2.1(d)], errors in $[\rho_w(\lambda)]_N$ for two NIR bands are also included. Results in Figure 2.1 show that, as SNR value increases (or noise decreases), error in $[\rho_w(\lambda)]_N$ decreases (as expected), and it reaches the inherent algorithm error [*Gordon and Wang*, 1994; *Wang*, 2007].

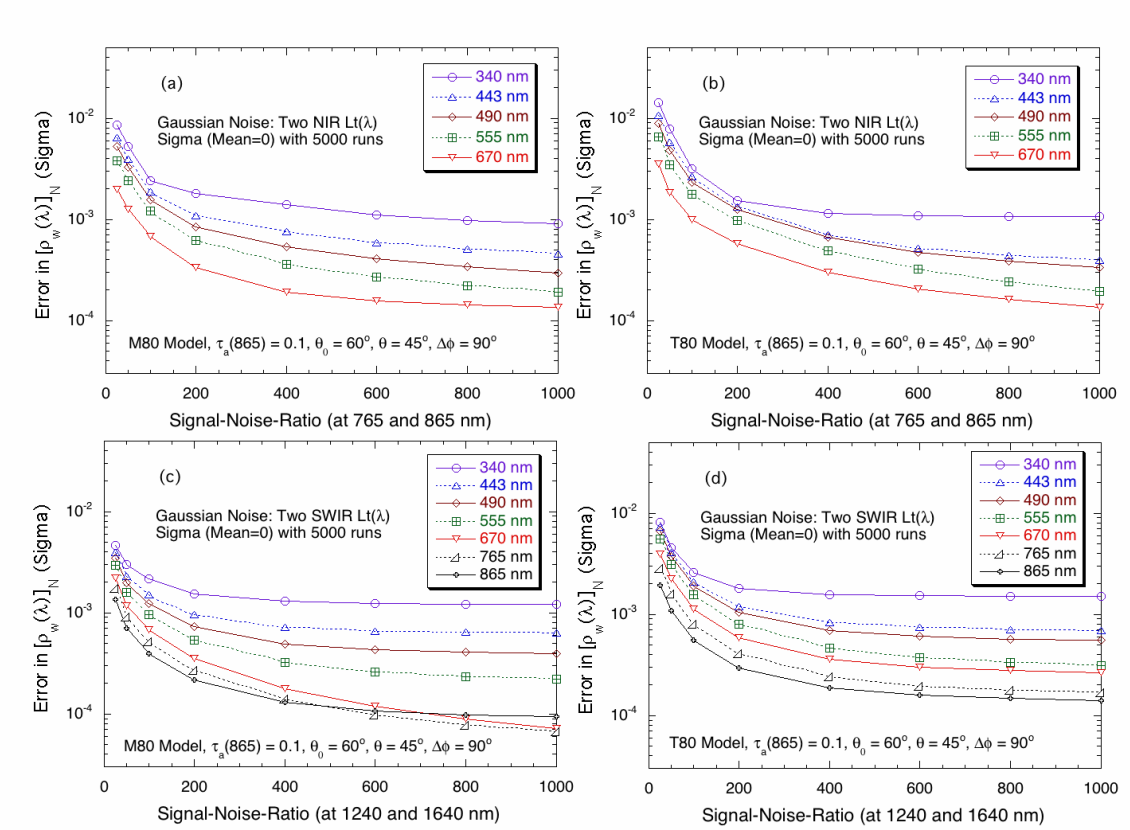

Figure 2.1. Error in the derived normalized water-leaving reflectance (in standard deviation with the mean value of 0) from 5000 Gaussian noise realizations as a function of the SNR value using the NIR (plots a and b) and SWIR (plots c and d) atmospheric correction algorithms. Aerosol model and AOT value, as well as solar-sensor geometry are indicated in each plot. For the NIR algorithm, error spectra data from UV to red are provided (plots a and b), while for the SWIR algorithm error spectra from UV to NIR are shown (plots c and d).

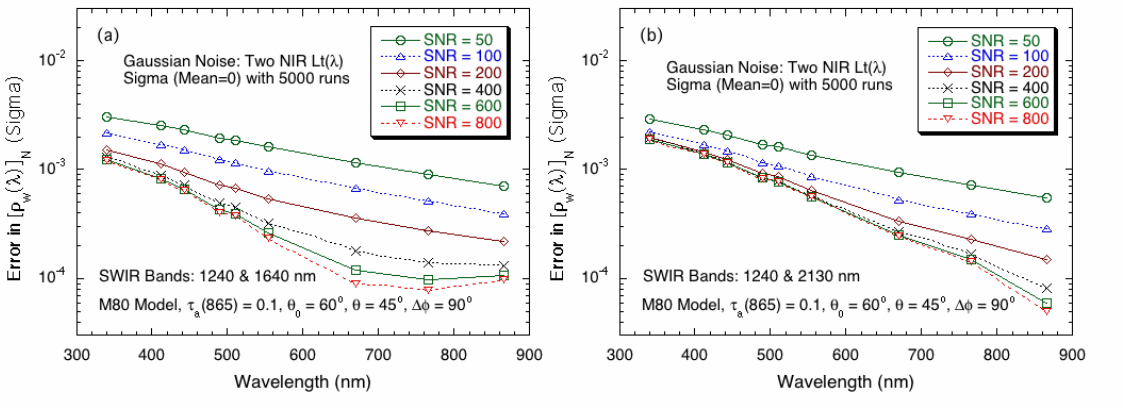

Figure 2.2. Error in the derived normalized water-leaving reflectance (in standard deviation with the mean value of 0) from 5000 Gaussian noise realizations as a function of the wavelength for various SNR values using the SWIR atmospheric correction algorithm with two SWIR bands of (a) 1240 and 1640 nm, and (b) 1240 and 2130 nm. Aerosol model and AOT value, as well as solar-sensor geometry are indicated in each plot.

Figure 2.2 provides sample results in the reflectance uncertainty spectra as a function of the wavelength (UV to NIR) for various SNR values with simulations from atmospheric correction algorithm using the two SWIR band sets, i.e., 1240 and 1640 nm (Figure 2.2(a)) and 1240 and 2130 nm (Figure 2.2(b)). Importantly, results in Figure 2.2 show that errors in $[\rho_w(\lambda)]_N$ from atmospheric correction are spectrally coherent. In addition, Figure 2.2 demonstrates that a SNR value between ~200-300 for the SWIR bands 1240 and 1640 nm is adequate (Figure 2.2(a)), while for the SWIR band 2130 nm a minimum of SNR value ~100 is required. At these SNR values for the SWIR bands, the derived water-leaving reflectance spectra from the SWIR atmospheric correction algorithms almost reach their corresponding algorithm inherent accuracy. It should be noted that, however, with even higher SNR values the derived $[\rho_w(\lambda)]_N$ at the red and NIR bands can be further improved.

Summary. Atmospheric correction and bio-optical simulations (see results from Stephane Maritorena) suggest that (1) for the NIR bands a minimum SNR value of ~600 is required, and (2) for the SWIR bands at 1240 and 1640 nm a minimum SNR value of ~200-300 is required, while for the 2130 nm band a minimum SNR value of ~100 is adequate.

2.3. Bio-optical model sensitivity analysis

Simulations were performed to assess how noise in the spectral marine remote sensing reflectance, Rrs(λ), affects the retrievals of biogeochemical variables from a semi-analytical ocean color model (GSM01, *Maritorena et al.* [2002]). These analyses were performed in order to assess the required SNRs in the ACE visible bands to ensure accurate bio-optical retrievals. Noise is created from the at-sea-level atmosphere reflectance spectra derived from the atmosphere specific simulations ran by Menghua Wang. The spectral atmospheric noise is added to a marine reflectance spectrum at the surface derived from a chlorophyll-based model [*Morel and Maritorena*, 2001]. We compared the model retrievals obtained when spectral reflectance is contaminated by noise to those retrieved from noise-free spectra. These simulations were run for a variety of atmospheric and marine conditions. This is briefly described below.

Two main kinds of noise were considered: 1) Atmospheric noise caused by errors in the NIR bands and propagated to the visible bands and, 2) noise as a random, spectrally uncoherent fraction of the Top-of-Atmosphere reflectance in addition to the NIR created noise. This latter case was designed to represent radiometric noise from other sources than the NIR bands (e.g. calibration). These two cases, will be referred to as "NIR" and "radiometric" errors, respectively.

In all runs, the "pure" marine Rrs signal (= no noise) is generated from the MM01 model [*Morel and Maritorena*, 2001] for 10 chlorophyll concentration (Chl) values in the 0.02-5 mg/m^3 range (400-700 nm every 5 nm). The GSM01 retrievals from the inversion of these "no noise" spectra are the reference to which the "noisy" NIR and radiometric cases are compared to.

For the "NIR" errors case, the at-sea-level reflectance spectra caused by errors in the NIR bands (from Menghua Wang) are converted to Rrs, $Rrs\_NIR(\lambda)$, and added to a MM01 marine spectrum, $Rrs\_MM01(\lambda, Chl)$, so

$$Rrs(\lambda, ocean) = Rrs\_MM01(\lambda, Chl) + Rrs\_NIR(\lambda) \quad [Eq\ 2.1]$$

The resulting spectrum, $Rrs(\lambda, ocean)$, is then inverted in GSM. The three GSM retrievals (Chl, CDM, b_{bp}) are then compared to the "no noise" case for 5000 spectra for each combination of SNR (8 values), AOT(865) and atmospheric model (2 models) and marine $Rrs(\lambda)$ (10 spectra). The comparisons are expressed in terms of the %rms for each of the GSM01 product and at each Chl level used to generate the marine Rrs. The %rms is defined as rms*100/reference (reference = retrieval in the no noise case).

For the "radiometric" errors case, a random, Gaussian, spectrally uncoherent fraction of a TOA signal is added to the marine spectra created similarly to what is described in the "NIR" case above. First, TOA signals are constructed for a black ocean with the M80 and T80 models, AOT(865) = 0.1 and for solar, sensor, and relative azimuth angles of 60, 45, and 90 degrees, respectively. The ocean contribution to the TOA signal is calculated as a MM01 reflectance spectrum transmitted through the atmosphere (with transmittance values matching the atmospheric model and geometry and AOT(865) of 0.05, 0.1, 0.2, and 0.3) and is added to the atmospheric TOA component (converted to Rrs units; $Rrs\_TOA(\lambda)$). The fraction of the TOA signal that is added to the marine spectrum created as in the NIR cases is determined through the generation of random Gaussian numbers with a mean of 0 and a standard-deviation of 1/SNR(visible) with SNR(visible) set to 10., 20., 40., 100., 200., 400., 800., 1000. and 2000. Then, each wavelength of the TOA spectrum is multiplied by a unique random number (rn) and that fraction of the TOA spectrum is added to the other components of the marine signal. This is done independently for each of the 5000 spectra corresponding to each SNR(NIR)/AOT(865)/atmospheric model combination used in the atmosphere simulations. In summary, in the "radiometric" errors case the at-sea-level Rrs is generated as:

$$Rrs(\lambda, ocean) = Rrs\_MM01(\lambda, Chl) + Rrs\_NIR(\lambda) + (Rrs\_TOA(\lambda) * rn(\lambda, SNR(visible)) \quad [Eq\ 2.2]$$

By looking at how much the retrievals from the noisy reflectance spectra depart from those derived without addition of noise, it is possible to assess the SNR(visible) value that allows an acceptable accuracy in the retrievals. It should be mentioned that in this approach, we assume an identical SNR level throughout the visible spectrum and does not take into account the fluorescence bands. Figures 2.3 and 2.4 illustrate the results of these analyses.

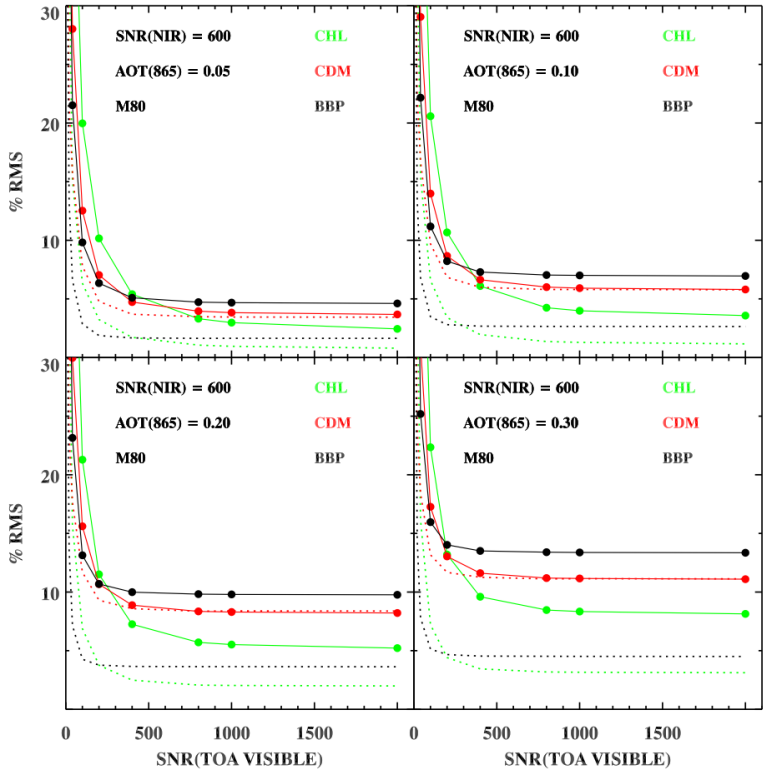

Figure 2.3. Example of the average (solid lines and symbols) and standard-deviation (dotted lines) of the %rms error over the full range of Chl values used as input in MM01 for the 3 GSM01 retrievals (green: Chl, red: CDM, black: b_{bp}) as a function of the SNR values in the visible and for SNR(NIR)=600 and different AOT(865) values.

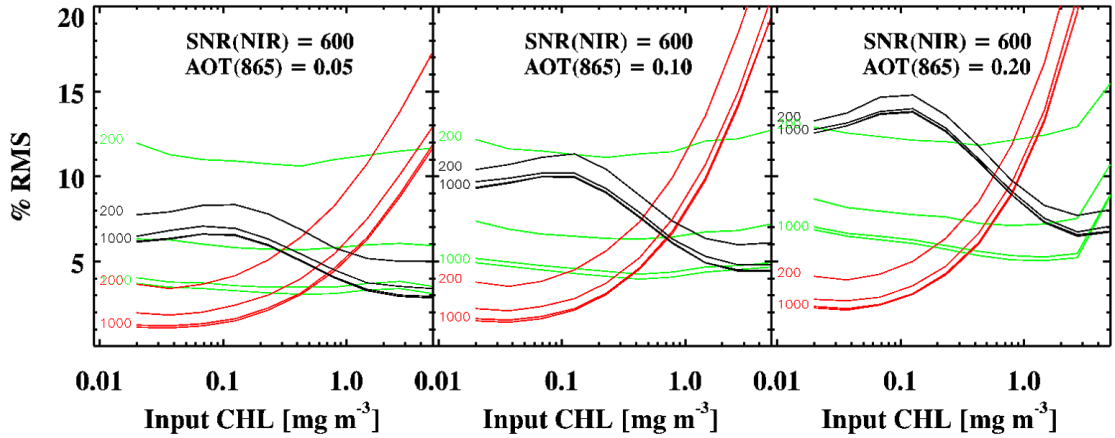

Figure 2.4. Example of the %rms error for each of the GSM01 retrievals (green: CHL, red: CDM, black: BBP) as a function of the CHL values used as input in MM01 for SNR(NIR)= 600 and different AOT(865) values. For each retrieval, the curves for SNR(visible) of 200, 400, 800 and 1000 are plotted, the highest (=1000) and lowest (=200) SNR(visible) values are indicated at either the beginning or the end of each curve.

For the minimum SNR(NIR) value of 600 suggested above, Figure 2.4 shows that for the three GSM retrievals the errors become stable in the 800-1000 SNR(vis) range (Chl gets stable at higher SNRs than the other 2 retrievals). The mean error (for the full range of Chl values used as input into MM01) remains under 10% for the clear atmosphere cases only (AOT(865) ≤ 0.1). This is confirmed in Figure 2.3 where the errors in the GSM retrievals stay under or close to 10% (except for CDM in eutrophic waters) for clear atmospheres and high SNRs. For the visible bands, a minimum SNR of ~1000 is thus recommended.

2.4. Measurement requirements summary

The ocean radiometer requirements are outlined in the following two tables. The first provides general sensor performance and mission support requirements. The second lists specific data on multispectral bands, bandwidths, typical clear sky top-of-atmosphere radiances over the ocean, saturation radiances, and minimum SNRs (based on the analyses above, Table 2.3). In Table 2.2, the SNR value at 350 nm is lower than in the other UV bands because its application for detecting absorbing aerosols does not require a value of 1000. Also, the SNR at 678 nm is set at 1400 based on analysis of MODIS retrievals (the bio-optical sensitivity analyses above did not include fluorescence line height). In the wavelength domain of 345-755 nm, multispectral bands are aggregations of 5 nm hyperspectral bands.

Table 2.2. General requirements for ocean radiometer and mission support

Radiometer Spectral Attributes	26 Spectral Bands (see Table 3)	10 nm fluorescence bands (667, 678, 710, 748 nm band centers)
		10 to 40 nm bandwidth aerosol correction bands at 748, 765, 865, 1245, 1640, 2135 nm
		820 nm band for estimation of column water vapor concentration
		350 nm band for absorbing aerosol detection
	5 nm resolution 345 to 755	Functional group derivative analyses
	Polarization	≤ 1% sensor radiometric sensitivity, ≤ 0.2% prelaunch characterization accuracy
	No saturation in multispectral bands	
Accuracy & Stability	Prelaunch radiance calibration accuracy	≤ 2%
	On-orbit vicarious calibration accuracy	≤ 0.2%
	Radiometric stability knowledge	≤ 0.1%, mission duration ≤ 0.1%, one-month prelaunch verification
Spatial Coverage	2-day global coverage	±58.3° cross-track swath
	1 km resolution at center of swath	
Other	±20° sensor tilt	Sunglint avoidance
	5 year minimum design lifetime	
	Monthly lunar imaging	7° phase angle through Earth-view sensor port

*Table 2.3. OES multispectral band centers, bandwidths (**∇λ**), typical top-of-atmosphere clear sky ocean radiances (Ltyp), saturation radiances (Lmax), and <u>minimum</u> SNRs at Ltyp. Radiance units are mW cm^{-2} μm^{-1} sr^{-1}.*

λ	∇λ	Ltyp	Lmax	SNR-spec
350	15	7.46	35.6	300
360	15	7.22	37.6	1000
385	15	6.11	38.1	1000
412	15	7.86	60.2	1000
425	15	6.95	58.5	1000
443	15	7.02	66.4	1000
460	15	6.83	72.4	1000
475	15	6.19	72.2	1000
490	15	5.31	68.6	1000
510	15	4.58	66.3	1000
532	15	3.92	65.1	1000
555	15	3.39	64.3	1000
583	15	2.81	62.4	1000
617	15	2.19	58.2	1000
640	10	1.90	56.4	1000
655	15	1.67	53.5	1000
665	10	1.60	53.6	1000
678	10	1.45	51.9	1400
710	15	1.19	48.9	1000
748	10	0.93	44.7	600
765	40	0.83	43.0	600
820	15	0.59	39.3	600
865	40	0.45	33.3	600
1245	20	0.088	15.8	250
1640	40	0.029	8.2	180
2135	50	0.008	2.2	100

GLOSSARY OF TERMS

a	Total Absorption Coefficient
a_{CDOM}	Colored Dissolved Organic Material Absorption Coefficient
ACE	Aerosol-Cloud-Ecosystem Mission
a_d	Detrital Absorption Coefficient
AOT	Aerosol Optical Thickness
a_{ph}	Phytoplankton Absorption Coefficient
b_b	Backscattering Coefficient
b_{bp}	Particulate Backscattering Coefficient
C	Carbon
c	Attenuation coefficient
CALIPSO	Cloud-Aerosol Lidar and Infrared Pathfinder Satellite Observation
CDM	Colored Dissolved and Detrital Material, see Maritorena et al. [2002]
CDOM	Colored Dissolved Organic Material
Chl	Chlorophyll
CLIVAR	World Climate Research Program Climate Variability
C_{phyto}	Phytoplankton Carbon Concentration
CZCS	Coastal Zone Color Scanner
DIC	Dissolved Innorganic Carbon
DOC	Dissolved Organic Carbon
Envisat	ESA Earth Observing Satelite
ϕ, FQY	Fluorescence Quantum Yield
FLH	Normalized Fluorescence Line-height
GOCECP	Global Ocean Carbon, Ecosystems, and Coastal Processes
GSFC	NASA Goddard Space Flight Center
GSM01	Semi-Analytical Ocean Color Model, Maritorena et al. [2002]
HAB	Harmful Algal Bloom
Kd(490)	Diffuse Attenuation Coefficient for Downwelling plane irradiance at 490 nm
Lmax	Top of Atmosphere Maximum Radiances
Ltyp	Top of Atmosphere Typical Radiances
M80	Maritime Aerosol Model
MERIS	Medium Resolution Imaging Spectrometer
ML	Mixed Layer
MLD	Mixed Layer Depth
MM01	chlorophyll-based optical model, Morel and Maritorena [2001]
MODIS	Moderate Resolution Imaging Spectroradiometer
NESDS	National Research Council Earth Sciences Decadal Survey
NIR	Near Infrared
$\nabla\lambda$	Bandwidth
NPP	Net Primary Production
OCB	Ocean Carbon and Biogeochemistry
OCEaNS	Ocean Carbon, Ecology and Near-Shore

OES	Ocean Ecosystem Spectroradiometer
OOI	Ocean Observatories Initiative
PACE	Plankton, Aerosol, Cloud, ocean Ecosystem
PAR	Incident Photosynthetically Available Radiation
PhyLM	Physiology-Multispectral Mission
PIC	Particulate Inorganic Carbon
POC	Particulate Organic Carbon
PSD	Particle Size Distribution
$[\rho_w(\lambda)]_N$	Normalized Water-Leaving Reflectance
rn	Unique random number
Rrs(l)	Remote Sensing Reflectance
Rrs_MM01 (λ, Chl)	Remote Sensing Reflectance derived following Morel and Maritorena [2001]
Rrs_NIR(λ)	Remote Sensing Reflectance caused by the errors in NIR bands
Rrs_TOA(λ)	Atmospheric component contributing to the Top of Atmosphere
SCIAMACHY	Scanning Imaging Absorption SpectroMeter for Atmospheric CHartographY
SeaBASS	SeaWiFS Bio-optical Archive and Storage System
SeaWiFS	Sea-Viewing Wide Field of View Sensor
SLC	*Synechococcus*-like cyanobacteria
SNR	Signal-to-Noise Ratio
SNR-spec	Minimum Signal To Noise Ratio at Top of Atmosphere typical Radiances
SOLAS	Surface Ocean-Lower Atmosphere Study
SQ	Science Question
SSH	Sea Surface Height
SST	Sea Surface Temperature
STD	Standard Deviation
SWIR	Shortwave Infrared
T80	Tropospheric Model
TChl-a	Total Chlorophyll-a concentration
TOA	Top Of Atmosphere
UV	Ultra-Violet
VIIRS	Visible Infrared Imaging Spectroradiometer
$Z_{1\%}$	1% Photosynthetically Available Radiation Depth
%rms	Root Mean Square, expressed as rms*100/reference

References

Alvain, S., C. Moulin, Y. Dandonneau, and F.-M. Bréon (2005), Remote sensing of phytoplankton groups in case 1 waters from global SeaWiFS imagery, *Deep Sea Res Part 1 Oceanogr Res Pap.*, *52*(11), 1989-2004, doi:10.1016/j.dsr.2005.06.015.

Bailey, S. W., B. A. Franz, and P. J. Werdell (2010), Estimation of near-infrared water-leaving reflectance for satellite ocean color data processing, *Opt. Express*, *18*(7), 7521-7527, doi:10.1364/OE.18.007521.

Balch, W. M., D. T. Drapeau, B. C. Bowler, and E. S. Booth (2007), Prediction of pelagic calcification rates using satellite measurements, *Deep Sea Research Part II: Topical Studies in Oceanography*, *54*(5), 478-495, doi:10.1016/j.dsr2.2006.12.006.

Balch, W. M., H. R. Gordon, B. C. Bowler, D. T. Drapeau, and E. S. Booth (2005), Calcium carbonate measurements in the surface global ocean based on Moderate-Resolution Imaging Spectroradiometer data, *J. Geophys. Res.*, *110*(C7), C07001, doi:10.1029/2004jc002560.

Behrenfeld, M. J., and E. Boss (2006), Beam attenuation and chlorophyll concentration as alternative optical indices of phytoplankton biomass, *J. Mar. Res.*, *64*(3), 431-451, doi:10.1357/002224006778189563.

Behrenfeld, M. J., E. Boss, D. A. Siegel, and D. M. Shea (2005), Carbon-based ocean productivity and phytoplankton physiology from space, *Global Biogeochem. Cycles*, *19*(1), GB1006, doi:10.1029/2004GB002299.

Behrenfeld, M. J., and P. G. Falkowski (1997), Photosynthetic rates derived from satellite-based chlorophyll concentration, *Limnol. Oceanogr.*, *42*(1), 1-20, doi:10.4319/lo.1997.42.1.0001.

Behrenfeld, M. J., K. H. Halsey, and A. J. Milligan (2008), Evolved physiological responses of phytoplankton to their integrated growth environment, *Philosophical Transactions of the Royal Society B: Biological Sciences*, *363*(1504), 2687-2703, doi:10.1098/rstb.2008.0019.

Behrenfeld, M. J., et al. (2009), Satellite-detected fluorescence reveals global physiology of ocean phytoplankton, *Biogeosciences*, *6*(5), 779-794, doi:10.5194/bg-6-779-2009.

Bracher, A., M. Vountas, T. Dinter, J. P. Burrows, R. Rottgers, and I. Peeken (2009), Quantitative observation of cyanobacteria and diatoms from space using PhytoDOAS on SCIAMACHY data, *Biogeosciences*, *6*(5), 751-764, doi:10.5194/bg-6-751-2009.

Bricaud, A., M. Babin, H. Claustre, J. Ras, and F. Tièche (2010), Light absorption properties and absorption budget of Southeast Pacific waters, *Journal of Geophysical Research: Oceans*, *115*(C8), n/a-n/a, doi:10.1029/2009JC005517.

Brown, C. W., and J. A. Yoder (1994), Coccolithophorid blooms in the global ocean, *Journal of Geophysical Research: Oceans*, *99*(C4), 7467-7482, doi:10.1029/93JC02156.

Carpenter, E. J. (1983), Nitrogen fixation by marine Oscillatoria (Trichodesmium) in the world's oceans, in *Nitrogen in the Marine Environment*, edited by E. J. Carpenter and D. G. Capone, pp. 65 - 103, Elsevier, New York.

Del Castillo, C. E., and R. L. Miller (2008), On the use of ocean color remote sensing to measure the transport of dissolved organic carbon by the Mississippi River Plume, *Remote Sens. Environ.*, *112*(3), 836-844, doi:DOI: 10.1016/j.rse.2007.06.015.

Deutsch, C., J. L. Sarmiento, D. M. Sigman, N. Gruber, and J. P. Dunne (2007), Spatial coupling of nitrogen inputs and losses in the ocean, *Nature*, *445*(7124), 163-167, doi:10.1038/nature05392.

Frouin, R., S. Nakamoto, A. Paci, A. Miller, and S. Iacobellis (2000), Biological modulation of sea surface temperature, *Proc. PORSEC, 2*, 498-501.

Gardner, W. D., A. Mishonov, and M. J. Richardson (2006), Global POC concentrations from in-situ and satellite data, *Deep-Sea Research Part Ii-Topical Studies in Oceanography*, *53*(5-7), 718-740, doi:DOI 10.1016/j.dsr2.2006.01.029.

Gervin, J., et al. (2002), Cost Analysis for a Recommended NASA Carbon Cycle Initiative, NASA/TM-2002-210007*Rep.*, 75 pp, NASA Goddard Space Flight Center, Greenbelt.

Goolsby, D. A. (2000), Mississippi Basin nitrogen flux believed to cause Gulf hypoxia, *Eos, Transactions American Geophysical Union*, *81*(29), 321-327, doi:10.1029/00EO00244.

Gordon, H. R., G. C. Boynton, W. M. Balch, S. B. Groom, D. S. Harbour, and T. J. Smyth (2001), Retrieval of coccolithophore calcite concentration from SeaWiFS Imagery, *Geophys. Res. Lett.*, *28*(8), 1587-1590, doi:10.1029/2000gl012025.

Gordon, H. R., and M. Wang (1994), Retrieval of water-leaving radiance and aerosol optical thickness over the oceans with SeaWiFS: a preliminary algorithm, *Appl. Opt.*, *33*(3), 443-452, doi:10.1364/AO.33.000443.

Gower, J., S. King, G. Borstad, and L. Brown (2005), Detection of intense plankton blooms using the 709 nm band of the MERIS imaging spectrometer, *Int. J. Remote Sens.*, *26* 2005–2012, doi:10.1080/01431160500075857.

Honjo, S. (1997), The rain of ocean particles and Earth's carbon cycle, *Oceanus*, 40(2), 4.

Huot, Y., A. Morel, M. S. Twardowski, D. Stramski, and R. A. Reynolds (2008), Particle optical backscattering along a chlorophyll gradient in the upper layer of the eastern South Pacific Ocean, *Biogeosciences*, *5*(2), 495-507.

IOCCG (2000), *Remote sensing of ocean colour in coastal, and other optically-complex, waters*, 140 pp., IOCCG Dartmouth, Canada.

IPCC (2007), Climate Change 2007: Synthesis Report. Contribution of Working Groups I, II and III to the Fourth Assessment Report of the Intergovernmental Panel on Climate Change*Rep*., 104 pp, IPCC, Geneva, Switzerland.

Kahru, M., and B. Mitchell (1998), Spectral reflectance and absorption of a massive red tide off southern California, *J. Geophys. Res.*, *103*(C10), 21601-21609, doi:10.1029/98JC01945.

Kahru, M., O. Savchuk, and R. Elmgren (2007), Satellite measurements of cyanobacterial bloom frequency in the Baltic Sea: interannual and spatial variability, *Mar. Ecol. Prog. Ser.*, *343*, 15-23, doi:10.3354/meps06943.

Kostadinov, T., D. Siegel, and S. Maritorena (2009), Retrieval of the particle size distribution from satellite ocean color observations, *Journal of Geophysical Research: Oceans*, *114*(C9), doi:10.1029/2009JC005303.

LaRoche, J., P. W. Boyd, R. M. L. McKay, and R. J. Geider (1996), Flavodoxin as an in situ marker for iron stress in phytoplankton, *Nature*, *382*, 802, doi:10.1038/382802a0.

Lee, Z., K. Carder, R. Arnone, and M. He (2007a), Determination of primary spectral bands for remote sensing of aquatic environments, *Sensors*, *7*(12), 3428-3441, doi:10.3390/s7123428.

Lee, Z., A. Weidemann, J. Kindle, R. Arnone, K. L. Carder, and C. Davis (2007b), Euphotic zone depth: Its derivation and implication to ocean-color remote sensing, *Journal of Geophysical Research-Oceans*, *112*(C3), doi:10.1029/2006JC003802.

Lee, Z. P., K. L. Carder, and R. A. Arnone (2002), Deriving inherent optical properties from water color: a multiband quasi-analytical algorithm for optically deep waters, *Appl. Opt.*, *41*(27), 5755-5772, doi:10.1364/AO.41.005755.

Lewis, M. R., M.-E. Carr, G. C. Feldman, W. Esaias, and C. McClain (1990), Influence of penetrating solar radiation on the heat budget of the equatorial Pacific Ocean, *Nature*, *347*(6293), 543-545, doi:10.1038/347543a0.

Loisel, H., J. M. Nicolas, A. Sciandra, D. Stramski, and A. Poteau (2006), Spectral dependency of optical backscattering by marine particles from satellite remote sensing of the global ocean, *Journal of Geophysical Research-Oceans*, *111*(C9), -, doi:10.1029/2005JC003367.

Longhurst, A. (1998), *Ecological Geography of the Sea*, Academic Press, San Diego, USA.

Mannino, A., M. E. Russ, and S. B. Hooker (2008), Algorithm development and validation for satellite-derived distributions of DOC and CDOM in the U.S. Middle Atlantic Bight, *J. Geophys. Res.*, *113*(C7), C07051, doi:10.1029/2007jc004493.

Maritorena, S., D. A. Siegel, and A. R. Peterson (2002), Optimization of a semianalytical ocean color model for global-scale applications, *Appl. Opt.*, *41*(15), 2705-2714, doi:10.1364/AO.41.002705.

Martin, J. H., and S. E. Fitzwater (1988), Iron deficiency limits phytoplankton growth in the north-east Pacific subarctic, *Nature*, *331*(6154), 341-343, doi:10.1038/331341a0.

McClain, C. R., et al. (2002), Science and Observation Recommendations for Future NASA Carbon Cycle Research, NASA/TM-2002-210009*Rep.*, 171 pp, NASA Goddard Space Flight Center, Greenbelt.

Moore, J. K., and O. Braucher (2008), Sedimentary and mineral dust sources of dissolved iron to the world ocean, *Biogeosciences*, *5*(3), 631-656, doi:10.5194/bg-5-631-2008.

Moore, J. K., S. C. Doney, K. Lindsay, N. Mahowald, and A. F. Michaels (2006), Nitrogen fixation amplifies the ocean biogeochemical response to decadal timescale variations in mineral dust deposition, *Tellus Series B-Chemical and Physical Meteorology*, *58*(5), 560-572, doi:10.1111/j.1600-0889.2006.00209.x.

Morel, A., Y. Huot, B. Gentili, P. J. Werdell, S. B. Hooker, and B. A. Franz (2007), Examining the consistency of products derived from various ocean color sensors in open ocean (Case 1) waters in the perspective of a multi-sensor approach, *Remote Sens. Environ.*, *111*(1), 69-88, doi:DOI 10.1016/j.rse.2007.03.012.

Morel, A., and S. Maritorena (2001), Bio-optical properties of oceanic waters: A reappraisal, *Journal of Geophysical Research-Oceans*, *106*(C4), 7163-7180, doi:10.1029/2000JC000319.

Muller-Karger, F. E., R. Varela, R. Thunell, R. Luerssen, C. Hu, and J. J. Walsh (2005), The importance of continental margins in the global carbon cycle, *Geophys. Res. Lett.*, *32*(1), doi:10.1029/2004GL021346.

Murtugudde, R., J. Beauchamp, C. R. McClain, M. Lewis, and A. J. Busalacchi (2002), Effects of penetrative radiation on the upper tropical ocean circulation, *J. Clim.*, *15*(5), 470-486.

NASA Ocean Biology and Biogeochemistry Working Group (2007), Earth's Living Ocean, The Unseen World, edited, p. 74.

NASA (2010), Responding to the Challenge of Climate and Environmental Change: NASA's Plan for a Climate-Centric Architecture for Earth Observations and Applications from Space, edited, p. 48.

Nelson, N. B., D. A. Siegel, C. A. Carlson, and C. M. Swan (2010), Tracing global biogeochemical cycles and meridional overturning circulation using chromophoric dissolved organic matter, *Geophys. Res. Lett.*, *37*(3), doi:10.1029/2009GL042325.

Ohlmann, J. C., D. A. Siegel, and C. Gautier (1996), Ocean mixed layer radiant heating and solar penetration: A global analysis, *J. Clim.*, *9*(10), 2265-2280, doi:10.1175/1520-0442(1996)009<2265:OMLRHA>2.0.CO;2.

Schlesinger, W. H. (1997), *Biogeochemistry: An Analysis of Global Change*, Second Edition ed., 588 pp., Academic Press, San Diego, San Francisco, New York, Boston, London, Sydney, Tokyo.

Shell, K., R. Frouin, S. Nakamoto, and R. Somerville (2003), Atmospheric response to solar radiation absorbed by phytoplankton, *Journal of Geophysical Research: Atmospheres*, *108*(D15), doi:10.1029/2003jd003440.

Siegel, D. A., S. Maritorena, N. B. Nelson, M. J. Behrenfeld, and C. R. McClain (2005), Colored dissolved organic matter and its influence on the satellite-based characterization of the ocean biosphere, *Geophys. Res. Lett.*, *32*(20), doi:10.1029/2005GL024310.

Siegel, D. A., S. Maritorena, N. B. Nelson, D. Hansell, and M. Lorenzi-Kayser (2002), Global distribution and dynamics of colored dissolved and detrital organic materials, *Journal of Geophysical Research: Oceans*, *107*(C12), doi:10.1029/2001JC000965.

Siegel, D. A., J. C. Ohlmann, L. Washburn, R. R. Bidigare, C. T. Nosse, E. Fields, and Y. Zhou (1995), Solar radiation, phytoplankton pigments and the radiant heating of the equatorial Pacific warm pool, *Journal of Geophysical Research: Oceans*, *100*(C3), 4885-4891, doi:10.1029/94JC03128.

Siegel, D. A., M. H. Wang, S. Maritorena, and W. Robinson (2000), Atmospheric correction of satellite ocean color imagery: the black pixel assumption, *Appl. Opt.*, *39*(21), 3582-3591, doi:10.1364/ao.39.003582.

Signorini, S. R., and C. R. McClain (2009), Effect of uncertainties in climatologic wind, ocean pCO2, and gas transfer algorithms on the estimate of global sea-air CO2 flux, *Global Biogeochem. Cycles*, *23*(2), n/a-n/a, doi:10.1029/2008GB003246.

Signorini, S. R., C. R. McClain, A. Mannino, and S. Bailey (2005), Report on Ocean Color and Carbon Study for the South Atlantic Bight and Chesapeake Bay Regions, NASA/TM-2005-212787*Rep.*, 45 pp, NASA Goddard Space Flight Center, Greenbelt.

Stramski, D., et al. (2008), Relationships between the surface concentration of particulate organic carbon and optical properties in the eastern South Pacific and eastern Atlantic Oceans, *Biogeosciences*, *5*(1), 171-201, doi:10.5194/bg-5-171-2008.

Takahashi, T., S. C. Sutherland, R. Wanninkhof, C. Sweeney, R. A. Feely, D. W. Chipman, B. Hales, G. Friederich, F. Chavez, and C. Sabine (2009), Climatological mean and decadal change in surface ocean pCO 2, and net sea–air CO 2 flux over the global oceans, *Deep Sea Research Part II: Topical Studies in Oceanography*, *56*(8), 554-577, doi:10.1016/j.dsr2.2008.12.009.

Tsunogai, S., S. Watanabe, and T. Sato (1999), Is there a "continental shelf pump" for the absorption of atmospheric CO2?, *Tellus B*, *51*(3), 701-712, doi:10.1034/j.1600-0889.1999.t01-2-00010.x.

Uitz, J., H. Claustre, A. Morel, and S. B. Hooker (2006), Vertical distribution of phytoplankton communities in open ocean: An assessment based on surface chlorophyll, *J. Geophys. Res.*, *111*(C8), C08005, doi:10.1029/2005jc003207.

Vountas, M., T. Dinter, A. Bracher, J. P. Burrows, and B. Sierk (2007), Spectral studies of ocean water with space-borne sensor SCIAMACHY using differential optical absorption Spectroscopy (DOAS), *Ocean Sci.*, *3*(3), 429-440, doi:10.5194/os-3-429-2007.

Walker, N. D., and N. N. Rabalais (2006), Relationships among satellite chlorophylla, river inputs, and hypoxia on the Louisiana Continental shelf, Gulf of Mexico, *Estuar Coasts*, *29*(6), 1081-1093, doi:10.1007/BF02781811.

Wang, M. (2007), Remote sensing of the ocean contributions from ultraviolet to near-infrared using the shortwave infrared bands: simulations, *Appl. Opt.*, *46*(9), 1535-1547, doi:10.1364/AO.46.001535.

Wang, M., and W. Shi (2005), Estimation of ocean contribution at the MODIS near-infrared wavelengths along the east coast of the US: Two case studies, *Geophys. Res. Lett.*, *32*(13), doi:10.1029/2005GL022917.

Werdell, P. J., B. A. Franz, and S. W. Bailey (2010), Evaluation of shortwave infrared atmospheric correction for ocean color remote sensing of Chesapeake Bay, *Remote Sens. Environ.*, *114*(10), 2238-2247, doi:10.1016/j.rse.2010.04.027.

Westberry, T., M. J. Behrenfeld, D. A. Siegel, and E. Boss (2008), Carbon-based primary productivity modeling with vertically resolved photoacclimation, *Global Biogeochem. Cycles*, *22*(2), doi:10.1029/2007GB003078.

Westberry, T., and D. A. Siegel (2006), Spatial and temporal distribution of Trichodesmium blooms in the world's oceans, *Global Biogeochem. Cycles*, *20*(4), doi:10.1029/2005GB002673.

Westberry, T., D. A. Siegel, and A. Subramaniam (2005), An improved bio-optical model for the remote sensing of Trichodesmium spp. blooms, *Journal of Geophysical Research: Oceans*, *110*(C6), doi:10.1029/2004JC002517.

Wiggert, J., R. Murtugudde, and J. Christian (2006), Annual ecosystem variability in the tropical Indian Ocean: Results of a coupled bio-physical ocean general circulation model, *Deep Sea Research Part II: Topical Studies in Oceanography*, *53*(5), 644-676, doi:10.1016/j.dsr2.2006.01.027.

Wynne, T., R. Stumpf, M. Tomlinson, R. Warner, P. Tester, J. Dyble, and G. Fahnenstiel (2008), Relating spectral shape to cyanobacterial blooms in the Laurentian Great Lakes, *Int. J. Remote Sens.*, *29*(12), 3665-3672, doi:10.1080/01431160802007640.

Yool, A., and M. J. Fasham (2001), An examination of the “continental shelf pump” in an open ocean general circulation model, *Global Biogeochem. Cycles*, *15*(4), 831-844, doi:10.1029/2000GB001359.